2006

Nature and completeness of galaxies detected in the Two Micron All Sky Survey

DH McIntosh

EF Bell

MD Weinberg
University of Massachusetts - Amherst

N Katz
University of Massachusetts - Amherst

Recommended Citation
McIntosh, DH; Bell, EF; Weinberg, MD; and Katz, N, "Nature and completeness of galaxies detected in the Two Micron All Sky Survey" (2006). *MONTHLY NOTICES OF THE ROYAL ASTRONOMICAL SOCIETY*. 39.
10.1111/j.1365-2966.2006.11115.x

Mon. Not. R. Astron. Soc. **000**, 1–19 (2005) Printed 5 February 2008 (MN LATEX style file v2.2)

Nature and completeness of galaxies detected in the Two Micron All Sky Survey

Daniel H. McIntosh[1⋆], Eric F. Bell[2], Martin D. Weinberg[1], and Neal Katz[1]
[1]*Department of Astronomy, University of Massachusetts, Amherst, MA 01003, USA*
[2]*Max Planck Institut für Astronomie, Königstuhl 17, D-69117 Heidelberg, Germany*

DRAFT: 5 February 2008

ABSTRACT
The *Two Micron All Sky Survey* (2MASS) provides the most comprehensive dataset of near-infrared galaxy properties. We cross correlate the well-defined and highly complete spectroscopic selection of over 156,000 bright ($r \leq 17.5$ mag) galaxies in the *Sloan Digital Sky Survey* (SDSS) Main Galaxy Sample (MGS) with 2MASS sources to explore the nature and completeness of the 2MASS (K-band) selection of nearby galaxies. Using estimates of total galaxy brightness direct from the 2MASS and SDSS public catalogues, corrected only for Galactic extinction, we find that 2MASS detects 90 percent of the MGS brighter than $r = 17$ mag. We quantify the completeness of 2MASS galaxies in terms of optical properties from SDSS. For $r \leq 16$ mag, 93.1% of the MGS is found in the 2MASS Extended Source Catalog (XSC). These detections span the representative range of optical and near-infrared galaxy properties, but with a surface brightness-dependent bias to preferentially miss sources at the extreme blue and low-concentration end of parameter space, which are consistent with the most morphologically late-type galaxy population. An XSC completeness of 97.5% is achievable at bright magnitudes, with blue low-surface-brightness galaxies being the only major source of incompleteness, if one follows our careful matching criteria and weeds out spurious SDSS sources. We conclude that the rapid drop in XSC completeness at $r > 16$ mag reflects the sharp surface-brightness limit of the extended source detection algorithm in 2MASS. As a result, the $r > 16$ galaxies found in the XSC are over-representative in red early types and under-representative in blue late types. At $r > 16$ mag the XSC suffers an additional selection effect from the $2-3''$ spatial resolution limit of 2MASS. Therefore, in the range $16 < r \leq 17$ mag, 2MASS continues to detect 90% of the MGS, but with a growing fraction found in the Point Source Catalog (PSC) only. Overall, one third of the MGS is detected in the 2MASS PSC but not the XSC. A combined $K \leq 13.57$ and $r \leq 16$ magnitude-limited selection provides the most representative inventory of galaxies in the local cosmos with near-infrared and optical measurements, and 90.8% completeness . Using data from the SDSS Second Data Release, this sample contains nearly 20,000 galaxies with a median redshift of 0.052.

Key words: surveys – galaxies: general – galaxies: fundamental parameters.

1 MOTIVATION

A detailed understanding of the galaxy population in the present-day universe is essential for constraining theories of galaxy formation and evolution. To this end, public resources have been dedicated to producing large comprehensive surveys of galaxies. Foremost among these are the *Two Micron All Sky Survey* (2MASS; Skrutskie et al. 1997), the *Sloan Digital Sky Survey* (SDSS; York et al. 2000), and the *Two-degree Field Galaxy Redshift Survey* (2dFGRS; Colless et al. 2001), which will remain cornerstones of galaxy characterisation for at least the next decade. 2MASS has mapped the near-infrared (near-IR) properties of more than 1.6 million galaxies over the entire sky, providing a large-scale view of the local universe minimally affected by dust, and a rich resource for understanding the full stellar mass component of $z \sim 0$ galaxies that is much less biased by young stellar light compared with optical surveys. The SDSS continues to acquire data and will ultimately cover roughly one quarter of the entire sky to a limiting depth considerably fainter than 2MASS. While each survey provides a wealth of measured galaxy properties, the ability to obtain representative samples of galaxies depends on a detailed assessment of each survey's selection effects and completeness. In this paper, we explore the 2MASS selection of local galaxies using the SDSS Main Galaxy Sample (MGS Strauss et al. 2002) criteria to define a very complete and well-understood parent sample for comparison.

⋆ E-mail: dmac@hamerkop.astro.umass.edu

Already the 2MASS Extended Source Catalog (XSC Jarrett et al. 2000) has been used to study the large-scale spatial distribution of galaxies in the local cosmos (Jarrett et al. 2000; Kochanek et al. 2003; Maller et al. 2003, 2005; Sivakoff & Saslaw 2005; Frith et al. 2005). Additionally, 2MASS has been combined with redshift surveys such as SDSS, 2dFGRS, and LCRS (Shectman et al. 1996) to quantify the near-IR luminosity and stellar mass distributions of the present-day galaxy population (Cole et al. 2001; Kochanek et al. 2001; Balogh et al. 2001; Bell et al. 2003a,b; Karachentsev & Kutkin 2005). Our understanding of the overall $z \sim 0$ galaxy population from these studies depends on the detailed nature of the 2MASS sample. For example, if 2MASS preferentially selects red early-type galaxies at all brightnesses, then the aforementioned results would contain a type-dependent bias.

In practice, the completeness of a sample is the fraction of sources of a given magnitude that are detected. The XSC meets the original 2MASS science requirements of greater than 90% completeness for the detection of galaxies brighter than $K < 13.5$ mag (Jarrett et al. 2000)[1]. The science requirements and initial tests for XSC completeness and reliability are recorded in the 2MASS Explanatory Supplement[2], and a useful summary of the findings is given in §2 of Maller et al. (2005). Cole et al. (2001) found 2MASS galaxies limited to $K < 13.2$ mag to be highly complete and not missing a significant fraction of low-surface-brightness systems. Furthermore, in an initial analysis based on the SDSS Early Data Release (Stoughton et al. 2002), we found that the XSC misses only 2.5% of the known galaxy population down to $K = 13.57$ dust-corrected Kron magnitudes (Bell et al. 2003b). These studies show 2MASS to be a statistically complete sample of all sources brighter than a fixed K-band limit. Nevertheless, there are reports of galaxy populations missed by 2MASS; e.g., low-luminosity emission-line galaxies are under-represented (Salzer et al. 2005). Also, Kannappan et al. (in prep) find roughly 40% of Nearby Field Galaxy Survey (Jansen et al. 2000) dwarfs fainter than $M_B = -18$ have no counterparts in the 2MASS XSC.

In this study, we show that the XSC of 2MASS provides a very representative sample of galaxies with well-defined completeness. In particular, we use over 156,000 MGS galaxies from the SDSS Second Data Release (DR2 Abazajian et al. 2004) with spectroscopic redshifts and precise optical properties to quantify the completeness of 2MASS-selected galaxies. We elect to use this earlier SDSS release and note that the large sample size and representative nature afforded by DR2 is more than sufficient for the analysis herein. Moreover, the SDSS data processing has not changed substantively in subsequent releases (Adelman-McCarthy & et al. 2005). In §2, we describe the galaxy samples drawn from SDSS and 2MASS, the relevant parameters we use from these public databases, and our method for constructing matched galaxy catalogues. We analyse the completeness of 2MASS-selected galaxies as a function of optical properties in §3. In §4, we discuss the nature of galaxies detected and missed by 2MASS, and we provide our conclusions in §5.

[1] This requirement includes caveats that $K < 13.5$ completeness is true only for sources with Galactic latitude $|b| > 20^\circ$ and free from stellar confusion. Note, we use K to denote the 2MASS K_s-band (or K short) throughout.

[2] http://www.ipac.caltech.edu/2mass/releases/allsky/doc/explsup.html

2 GALAXY SAMPLES

For a detailed assessment of the completeness and nature at visible wavelengths of galaxies found in 2MASS, we require an optical survey that has enough sky coverage to sample a representative set of galaxies averaged over all environments, and has a limiting magnitude that is deeper than 2MASS so that we can construct samples of galaxies 2MASS does and does not detect. The SDSS meets these requirements and includes a suite of photometric and spectroscopic quantities, including redshifts, for the $> 99\%$ complete and uniform "main" spectroscopic selection of galaxies (MGS; Strauss et al. 2002). As such, the MGS is an ideal parent sample to test the completeness of 2MASS-selected galaxies, quantified by apparent and intrinsic optical properties. In this section we outline the relevant aspects of the 2MASS and SDSS galaxy samples, and our selection of combined samples. We include galaxies detected as point sources by 2MASS, and we separate these from extended sources in the following analyses.

2.1 SDSS Main Galaxy Sample

The SDSS is surveying a significant portion of the sky at latitudes outside of the Galactic plane where the effects of dust on optical properties are minimal. The SDSS provides deep ($r = 22.2$ mag limit) photometry from imaging in five optical passbands ($ugriz$) and follow-up spectroscopy for the brighter subset of galaxies. The target selection algorithm for the MGS is detailed in Strauss et al. (2002). Briefly, useful sources with $> 5\sigma$ detection were separated into stars and galaxies. The MGS includes all galaxies with r-band Petrosian magnitudes of $r \leq 17.77$, corrected for foreground Galactic extinction following Schlegel et al. (1998). A further surface brightness limit of $\mu_{50,r} = 23.0$ mag/arcsec^2 (see §2.3 for $\mu_{50,r}$ definition), retains 99% of the galaxies with $r \leq 17.77$ mag. The SDSS galaxy photometry is based on the Petrosian system, which allows an estimate of the total flux of each galaxy roughly independent of surface brightness. Recent studies give prescriptions that attempt to correct these estimates to the actual total (Graham et al. 2005), but here we elect to leave the SDSS magnitudes uncorrected. Our analysis is intimately tied to the MGS selection, which is based on Petrosian magnitudes direct from the public database, corrected only for Milky Way dust.

Using the SDSS Catalog Archive Server, we select 319,224 galaxies from the DR2 photometry database meeting the MGS magnitude and surface brightness cuts, with the following additional criteria: good (status & 0x2 > 0), primary (mode=1) sources flagged as galaxies (PrimTarg & 0x1c0 > 0; i.e., GALAXY or GALAXY_BIG or GALAXY_BRIGHT_CORE, as defined in Table 27 of Stoughton et al. 2002) [3]. The spectroscopic targeting was designed to meet its completeness specifications at $r \leq 17.77$ mag, but in practice this limit varies[4] between 17.50 and 17.77; therefore, for statistically representative samples a conservative limit of $r \leq 17.5$ mag is recommended (Abazajian et al. 2003). We employ this cut resulting in a sample of 228,645 galaxies with a high degree of completeness. We further remove all 943 (88) sources

[3] The PrimTarg flag is set to GALAXY by the image deblender when the MGS criteria are met including star/galaxy separation, and a number of fiber magnitude cuts designed to reject bright stars and very bright sources that can contaminate adjacent fiber spectra; Strauss et al. (2002).

[4] Spectroscopic targets were selected based on initial processing of the data resulting in subtle changes in the r-band flux limit and slight variations in the completeness limit over large angular scales.

with $(g-r)_{\rm mod} > 2.5$ (< -0.5) colours. Visual inspection of the SDSS images shows that these colour cuts remove defective and contaminated sources. In particular, the red cut sources are satellite trails and other defects (e.g., false detections) at $r \leq 15.5$, and roughly half defects and half point-like contamination at fainter magnitudes. The blue removed sources are 100% ($> 75\%$) point sources at $r \leq 16.5$ ($16.5 < r \leq 17.5$). We are left with a magnitude-limited sample of 227,614 galaxies with DR2 photometric properties; we call this our MGSphot-only sample.

Next, from the DR2 spectroscopic database we select the subset of MGSphot-only sources that have useful redshifts[5] (zConf>0.35). This is our primary parent sample of 156,788 galaxies with photometric properties and reliable redshifts, and represents the magnitude-limited ($r \leq 17.5$) MGS from DR2; we denote this sample MGSphot+spec. We stress that the large number difference between the MGSphot+spec and MGSphot-only samples is the result of the smaller effective coverage of the DR2 spectroscopic area as compared to the imaging footprint. A complex tiling algorithm was designed for the spectroscopic survey (Blanton et al. 2003) to provide nearly uniform completeness when sampling the non-uniform large-scale galaxy distribution of the local universe. For SDSS, this tiling samples $92-93\%$ of all targets, with the incomplete coverage owing to multiple objects within the $55''$ minimum fiber separation of the SDSS multi-object spectrograph (i.e., "fiber collisions"). This leads to a slight systematic under representation in regions of high galaxy number density (Hogg et al. 2004). For our purpose we are concerned with the completeness and representative nature of the overall sample, and therefore, a detailed accounting of MGS completeness as a function of position is not required.

Overall, the SDSS spectroscopic survey is 90% complete (Blanton et al. 2003; Hogg et al. 2004), with 7% incompleteness owing to fiber collisions as described above, and additional sources of incompleteness from bright star contamination (2%) and spectra with incorrect or impossible to determine redshifts (1%). The effective sky coverage of the DR2 spectroscopy is 2627 square degrees (Abazajian et al. 2004). If we extend the magnitude cut to $r = 17.77$, we obtain 209,730 MGS sources with redshifts, or 79.84 deg^{-2}. This is in good agreement with the expected surface density of ≈ 80 deg^{-2} from the MGS targeting of ≈ 90 deg^{-2} with a completeness of 90%, less an additional 1% from the $\mu_{50,r} > 23.0$ mag/arcsec^2 cut.

Finally, we note that two effects cause the MGS spectroscopic sample to become noticeably incomplete for galaxies brighter than $r = 14.5$ mag: (i) to avoid excessive cross-talk and/or saturation in the spectrograph detectors, some targets were rejected if any pixels exceeded a peak flux level; and (ii) the image deblending software sometimes over deblended galaxies with large angular extent (Strauss et al. 2002). We performed a preliminary examination of this issue by using 2MASS to identify the locations of all large bright galaxies missed by the pipeline processing in a 710 deg^2 region (54% of spectroscopic coverage) of the SDSS First Data Release (Abazajian et al. 2003). We found that the MGS had no detection for $> 20\%$ and $> 50\%$ of XSC sources brighter than $K = 11.5$ and $K = 9.5$ mag, respectively. From a typical colour of $(r-K) \approx 3$ (e.g., Fukugita et al. 1995), these K limits correspond roughly to $r = 14.5$ and $r = 12.5$ mag. Yet, the MGS did not preferentially miss or detect galaxies of one morphological type (visually early or late) over another. Therefore, the bright end of the MGS remains representative. Furthermore, we note that an $r \leq 14.5$ mag cut contains 1.5% of the total $r \leq 17.5$ MGS; therefore, bright galaxy incompleteness only affects our overall completeness at the $< 1\%$ level. Throughout this work, our determinations of 2MASS completeness are with respect to the MGS, limited only at the faint end ($r = 17.5$). We will address this issue in more detail in a subsequent paper.

[5] This value for the redshift confidence is suggested in the following DR2 website: http://www.sdss.org/dr2/products/spectra/index.html. We note that Stoughton et al. (2002) used a cut of zConf≥ 0.6 for "high" redshift confidence. The difference between these two cuts amounts to only 10 galaxies.

2.2 2MASS Extended and Point Source Catalogs

2MASS is an all-sky survey with uniform photometry in the near-IR JHK ($1.15, 1.65, 2.15\mu$m) passbands. The 2MASS analysis pipeline uses well-defined selection criteria to separate extended and point sources. The pipeline and XSC construction are described in detail in Jarrett et al. (2000). The photometric calibration and uniformity of 2MASS is quantified in Nikolaev et al. (2000).

The PSC provides magnitudes for 188 million sources brighter than $K = 14.3$ mag, the 10σ point-source sensitivity limit. At this magnitude limit, the PSC meets the 2MASS science requirement of 99% completeness (see the Explanatory Supplement). PSC magnitudes given in $8''$ diameter apertures (k_m_stdap) provide a rough total brightness for unresolved galaxies. In Bell et al. (2003b), we showed that PSC aperture magnitudes for galaxies fainter than $K = 13.5$ have rather large systematic offsets of -0.85 mag (0.3 mag rms). We do not recommend using the PSC for precise photometric studies of galaxies, but we include PSC detections in this analysis to provide a complete picture of 2MASS galaxy selection.

The XSC contains over 750,000 galaxies brighter than $K = 13.5$ mag. As described in §1, at this magnitude limit the XSC meets the 2MASS science requirement of at least 90% galaxy completeness for the Galactic latitudes ($|b| > 20^\circ$) covered by SDSS. In addition, within these limits the XSC is at least 98% reliable; i.e., it contains true extended astronomical objects. The automated processing of the XSC produces systematically incomplete photometry for the small subset of galaxies larger than $50''$ owing to the typical 2MASS scan width of $8.5'$ (Jarrett et al. 2000). For our analysis, we include the 2MASS Large Galaxy Atlas (Jarrett et al. 2003) sample of 540 galaxies flagged (cc_flag='Z') in the XSC database, which was assembled to account for most of the scan size photometric incompleteness.

2MASS employs the Kron (1980) system to define total galaxy magnitude in a fiducial elliptical aperture with semi-major axes equal to 2.5 times the first moment of the brightness distribution. The first moment calculation is computed to a radius that is five times the J-band 20 mag/arcsec^2 isophote and is limited to a minimum of $5''$ because the point-spread function (PSF) dominates the surface brightness profile within this radius (see the 2MASS Explanatory Supplement for details). Throughout this paper all 2MASS photometry will be cited in extinction-corrected Kron magnitudes. As a result of the short exposure times (7.8 s with a 1.3-m telescope), 2MASS Kron magnitudes systematically underestimate the true total flux by ≈ 0.1 mag (Cole et al. 2001; Bell et al. 2003b). The purpose of this work is to describe the galaxy content of the publicly-available 2MASS data; thus, throughout we do not correct apparent near-IR magnitudes for the missed flux. We note that we do consider this correction when estimating k-corrections (see §2.3).

2.3 Optical and Near-IR Quantities

Besides the Petrosian and Kron measures of total apparent magnitude discussed previously, we use additional optical and near-IR quantities in our analysis. We quantify galaxy colour using $(J-K)$ Kron magnitudes and $(g-r)$ model magnitudes. The SDSS includes model magnitudes for all five passbands measured consistently with the same aperture, which is determined by the best-fit model (either a de Vaucouleurs or an exponential radial profile) to the r-band image with PSF convolution. Colours based on these model magnitudes are recommended for galaxy studies (Abazajian et al. 2004).

The spectroscopic redshifts from the SDSS allow us to calculate rest-frame total luminosities and colours, k-corrected to redshift zero. We assume $H_0 = 70\,\mathrm{km\,s^{-1}\,Mpc^{-1}}$, $\Omega_M = 0.3$, and $\Omega_\Lambda = 0.7$. We estimate k-corrections using the method described by Bell et al. (2003b). Briefly, we fit a grid of non-evolving stellar population models (PÉGASE FIOC & ROCCA-VOLMERANGE 1997), with a range of metallicities and star formation histories of the form $\Psi \propto \exp(-t/\tau)$, to the optical and near-IR photometry of each galaxy and derive the k-correction from the best-fit template. Here, Ψ is the star formation rate and τ is the e-folding timescale, and the star formation starts at $z_{\rm initial} = 4$. For the optical photometry, we adopt Petrosian gri magnitudes and use model colours to estimate higher signal-to-noise u and z magnitudes: $u' = r + (u-r)_{\rm mod}$ and $z' = r + (z-r)_{\rm mod}$. When near-IR photometry is available (i.e., for galaxies with 2MASS detections), we apply a uniform offset of -0.1 magnitude to J and K to bring the 2MASS Kron magnitudes into agreement with magnitudes from deeper J and K-band data, following Cole et al. (2001) and Bell et al. (2003b). As already stated, we correct all magnitudes, luminosities, and colours for foreground reddening using the Galactic dust map of Schlegel et al. (1998). The mean and rms extinction corrections for the data we analyse here are -0.099 ± 0.071 (r-band), -0.013 ± 0.009 (K-band), -0.038 ± 0.027 ($g-r$), and -0.019 ± 0.014 ($J-K$) mag.

We include further galaxy structural properties in this analysis. The SDSS and 2MASS databases each provide measures of galaxy orientation given by the axis ratio (b/a): 2MASS measures $(b/a)_K$ from an elliptical fit to the 3σ isophote in the K-band image, whereas from SDSS we take the average r-band axis ratio $\langle b/a \rangle_r$ from values derived from the pure de Vaucouleurs and pure exponential model fits to the light profile. SDSS provides circular radii $\mathrm{r}_{90,r}$ and $\mathrm{r}_{50,r}$ that contain 90% and 50% of the Petrosian flux, respectively. The 2MASS XSC contains elliptical half-light sizes $\mathrm{a}_{50,K}$ measured along the major axis; therefore, for consistency we calculate the circularised K-band radius $\mathrm{r}_{50,K} = \mathrm{a}_{50,K}\sqrt{(b/a)_K}$. In turn, the sizes can be used to calculate various quantities such as the concentration index $c_r = \mathrm{r}_{90,r}/\mathrm{r}_{50,r}$, which is a measure of the degree of central concentration in the r-band galaxian light profile. In addition, within the half-light radii we have average surface brightnesses $\mu_{50,r} = r + 2.5\log_{10}(2\pi \mathrm{r}^2_{50,r})$ and $\mu_{50,K} = K + 2.5\log_{10}(2\pi \mathrm{r}^2_{50,K})$. We calculate physical sizes at each redshift from the angular diameter distance and our assumed cosmological parameters.

2.4 Combining Galaxy Detections From 2MASS and SDSS

We cross correlate the positions of our MGS-based samples with the XSC and PSC from 2MASS. For matching to the 2MASS XSC, we employ an optimum set of criteria (see Appendix A) that minimises contamination from multiple and random matches. We look for PSC matches only for those remaining MGS galaxies not detected in the XSC using a simple criteria of closest match within a $2''$ radius. The mean and rms angular separations between 2MASS and SDSS galaxy positions are $0.45''$ and $0.22''$ for the XSC, and $0.35''$ and $0.29''$ for the PSC. The absolute astrometric accuracies are $0\farcs5$ rms for 2MASS (Jarrett et al. 2000) and $< 0\farcs1$ rms for SDSS with $r < 20$ mag (Pier et al. 2003).

This cross correlation provides three subsamples of our main parent sample of 156,788 MGSphot+spec galaxies with DR2 spectroscopic measurements: (1) 89,742 galaxies with 2MASS extended source matches (and therefore have $ugrizJK$ total galaxy fluxes, plus optical and near-IR properties), (2) 51,716 with 2MASS point source counterparts (thus have $ugrizJK$ fluxes and optical properties), and (3) 15,330 without any 2MASS source matches (thus optical data only). Likewise, we find the following subsets from the cross correlation of the MGSphot-only sample ($N = 227,614$ galaxies) with 2MASS: (4) 130,348 matched to XSC, (5) 73,335 matched to PSC, and (6) 23,931 without any 2MASS counterparts. A further 2MASS completeness cut of $K \leq 13.57$ to subsample (1) results in 43,663 galaxies – the largest complete sample of galaxies with optical and near-IR photometric properties and reliable redshift measurements to date. We plot the redshift distributions of 2MASS extended sources with spectroscopic identification from DR2 in the upper right panel of Figure 6. The median redshift of the $K \leq 13.57$ sample is $z_{\rm med} = 0.076$, compared with $z_{\rm med} = 0.104$ for the MGS to $r \leq 17.77$ mag (Strauss et al. 2002); we find the MGS cut at $r = 17.5$ mag has $z_{\rm med} = 0.092$.

With the set of fundamental optical properties provided by SDSS, we compare the MGSphot-only and MGSphot+spec parameter distributions in Table 1. In terms of mean, RMS, and median of each optical parameter distribution, the main photometric sample and the subset with spectroscopy appear indistinguishable. In Figure 1, we plot the r magnitude distributions for the MGSphot-only, MGSphot+spec, and corresponding subsamples. In general, we see that the XSC detects most MGS galaxies brighter than $r = 16$ mag, that much of the fainter MGS sources are detected in the 2MASS PSC, and that the galaxies not detected by 2MASS are typically faint ($r > 16$ mag). We note that MGS nondetections brighter than $r = 16$ are unrelated to the 2MASS scanning geometry (see Fig. 2). Nevertheless, Figure 1 is not very illuminating in regards to the details of which galaxies 2MASS detects as extended or point sources, or not all.

In Figure 3, we show the r-magnitude "completeness function" (CF) for each subsample of MGSphot-only and MGSphot+spec. For example, the XSC (red) r-magnitude CF is given by the number of XSC-MGS matches divided by the total number of MGS sources in bins of $\Delta r = 0.1$ mag. We further quantify the completeness of 2MASS-detected galaxies in §3.1 by analysing the CFs relative to the MGS using additional optical properties. Relative to MGSphot-only, the 2MASS XSC appears $\geq 10\%$ incomplete at all r magnitudes, with systematically increasing incompleteness with increasing brightness. Yet, when considering spectroscopically-confirmed galaxies, the r-mag CF of the XSC shows that 2MASS galaxy detections are $> 90\%$ complete in every magnitude bin down to $r = 16$. If we include the galaxies detected in the PSC, the overall galaxy detection completeness of 2MASS using the MGSphot+spec sample remains $> 90\%$ for all $r \leq 17$ mag bins, and $> 80\%$ for bins in the range $17.0 < r \leq 17.5$ mag.

The incompleteness of 2MASS in the MGSphot-only sample at bright r magnitudes appears to be from sources not de-

tected in 2MASS in either the XSC or the PSC. This is surprising given that the 2MASS XSC is reported to be 97.5% complete for bright ($K \leq 13.57$ mag) sources (Bell et al. 2003b). To ascertain the nature of this apparent incompleteness, we visually inspect SDSS images of the 346 unmatched MGSphot-only sources with $r \leq 14.5$ mag and find that only a small fraction (13%) are actual bright galaxies. The vast majority (193) of these unmatched, bright SDSS photometric sources are imaging artifacts from luminous stars (e.g., diffraction spikes, scattered light). An additional 109 are false detections, the result of scattered halo light from nearby large galaxies or the overdeblending of large galaxies. The small number of $r \leq 14.5$ SDSS galaxies without 2MASS counterparts have large angular sizes and thus have very low apparent surface brightness. As shown in Figure 4, typical examples of these low-surface-brightness galaxies (LSBs) appear in 2MASS K-band images but are below the detection pipeline threshold. We note that if we correct the MGSphot-only r mag distribution above $r = 14.5$ mag for the 302 artifacts and false detections, then the fraction of bright SDSS galaxies with XSC matches (3421/3621) agrees with that found for the MGSphot+spec XSC subsample (95%).

For the rest of this analysis we will use the MGSphot+spec ($\equiv$ MGS) as the parent sample for describing the completeness of 2MASS-selected galaxies. This choice circumvents the artifact contamination shown above for MGSphot-only, and provides redshift information and spectroscopic confirmation for each galaxy. It is important to demonstrate the representative nature of 2MASS galaxies within the DR2 region and the $K \leq 13.57$ mag limit, where the XSC is required to be 90% complete and 98% reliable. In Figure 5, we compare the 2MASS near-IR property distributions for 43,663 XSC galaxies that have MGSphot+spec counterparts and 548,132 objects from the XSC with $|b| > 20^\circ$ and $0.1 \leq (J-K) \leq 2.5$. Note, the additional colour cut excludes 201 sources that are likely to be high-latitude Milky Way extended emission. We do not compare galaxies at fainter magnitudes, where 2MASS becomes increasingly nonuniform, unreliable, and incomplete. We see that the K-magnitude-limited samples have nearly identical K, $(J-K)$, $\mu_{50,K}$, and $(b/a)_K$ relative distributions. There is a small $(J-K)$ difference such that slightly more red galaxies are found in the MGS region than the overall sky above and below the Galactic plane. Following the same procedure as in Bell et al. (2003b), we find that the density of $10.0 < K < 13.5$ XSC sources in the DR2 spectroscopic coverage area is $n_{\rm gal} = 17.94 {\rm deg}^{-2}$, or 1.1% larger than the sky outside of the Milky Way plane. We expect that the slight red galaxy excess results from the small overdensity of DR2. The disagreement of completeness in XSC matches to bright MGS sources seen in Figure 3 is the result of differences in the MGSphot-only and MGSphot+spec selection rather than that of 2MASS.

Table 1. Comparison of MGSphot-only and MGSphot+spec parameter distributions.

	MGSphot-only			MGSphot+spec		
Parameter	mean	rms	median	mean	rms	median
r (mag)	16.73	0.74	16.96	16.75	0.72	16.97
c_r	2.64	0.42	2.65	2.64	0.41	2.65
$(g-r)$ (mag)	0.81	0.26	0.84	0.81	0.25	0.84
$\mu_{50,r}$ (mag/arcsec^2)	20.75	0.83	20.76	20.76	0.78	20.77
$r_{50,r}$ (arcsec)	2.82	1.69	2.46	2.77	1.40	2.46
$(b/a)_r$	0.63	0.21	0.67	0.64	0.21	0.67
z				0.097	0.051	0.092

Characteristics (mean, RMS, and median) of the parameter distributions from the MGSphot-only ($N = 227,614$ galaxies) and the MGSphot+spec ($N = 156,788$ galaxies) samples.

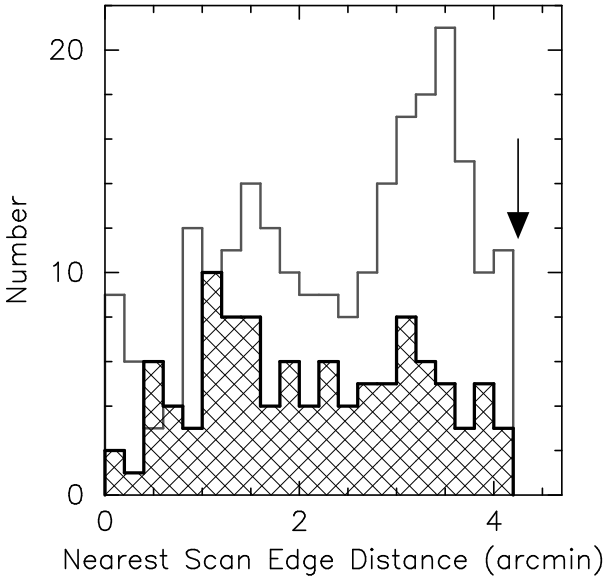

Figure 2. Distribution of distances from the nearest image scan edge for bright MGSphot+spec sources not detected by 2MASS in either the XSC or PSC. Each 2MASS scan is $8.5' \times 6^\circ$, thus, the maximum distance to the nearest edge is $4.25'$ as shown by the arrow. We plot all $r \leq 15$ (hatched), and a random half of the $15 < r \leq 16$ (dark grey outline), nondetections separately. Bright sources missed by 2MASS are uncorrelated with the scan boundaries.

3 2MASS GALAXY COMPLETENESS

We now use the SDSS main spectroscopic sample to explore the completeness of 2MASS galaxies in more detail. Recall that from the 156,788 $r \leq 17.5$ mag galaxies from the MGSphot+spec, we match 89,742 in the XSC and 51,716 in the PSC, leaving 15,330 without 2MASS counterparts. In Figure 6, we quantify the completeness of 2MASS-selected galaxies as a function of six optical observables: (from left to right) r-band concentration c_r, $(g-r)$ model colour, average half-light surface brightness $\mu_{50,r}$, half-light radius $r_{50,r}$, mean axis ratio $\langle b/a \rangle_r$, and spectroscopic redshift z. In the upper row we plot the total distributions for each property. The black histogram shows the MGSphot+spec sample, the 2MASS matches are in red (XSC) and green (PSC), and the blue histogram plots SDSS galaxies not detected by 2MASS. In the lower rows of Figure 6, we give the 2MASS galaxy CFs for each property split into four r magnitude bins each with the following minimum XSC completeness per bin from inspection of Figure 3: 95% ($r \leq 15.0$), 90% ($15.0 < r \leq 16.0$), 50% ($16.0 < r \leq 17.0$), and 10% ($17.0 < r \leq 17.5$). For this analysis the most important completeness pertains to galaxies detected in the XSC (thick red line), which provides a set of well-defined galactic parameters at near-IR wavelengths. We also show the CFs for the PSC (green) and unmatched (blue) galaxies in each r mag bin. The CFs for each subsample demonstrate and quantify the selection effects of galaxy detection by 2MASS; therefore, it is useful to think of the CFs as selection functions. The thin red line represents the CF for XSC

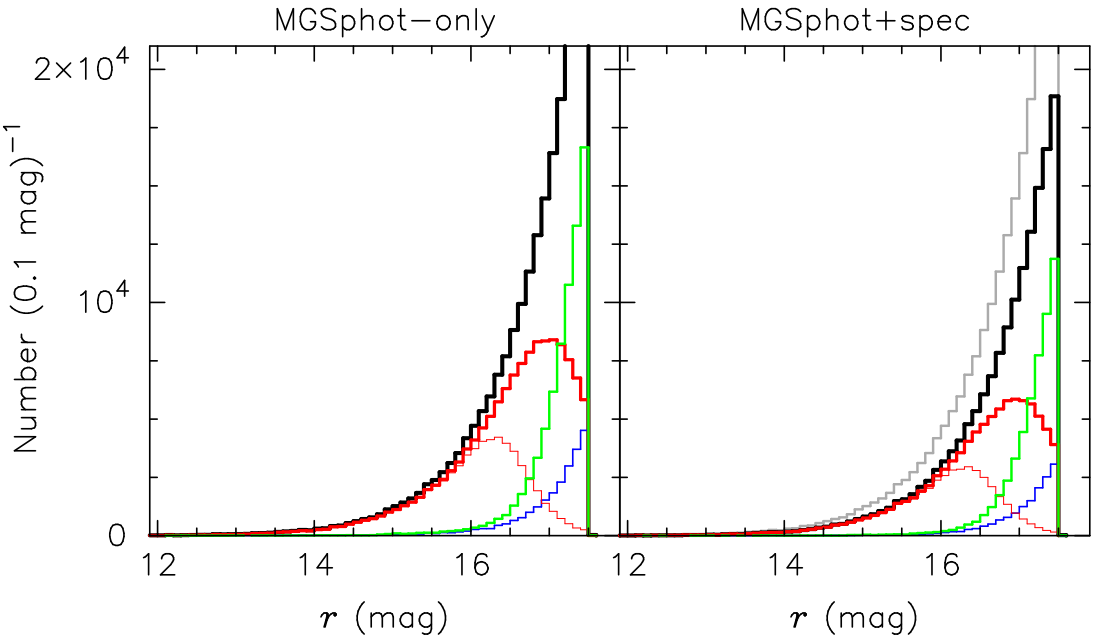

Figure 1. Apparent r-band Petrosian magnitude distributions (black) for the MGSphot-only ($N = 227,614$) and MGSphot+spec ($N = 156,788$) primary samples selected from DR2 and limited to $r \leq 17.5$ mag. In each panel, we show the related subsamples from our cross correlation with the 2MASS XSC (red) and PSC (green); sources without 2MASS counterparts are shown in blue. For comparison, we plot the MGSphot-only distribution in grey in the right panel. Thin red lines denote $K \leq 13.57$ magnitude-limited XSC samples. All magnitudes are corrected for Galactic extinction following Schlegel et al. (1998).

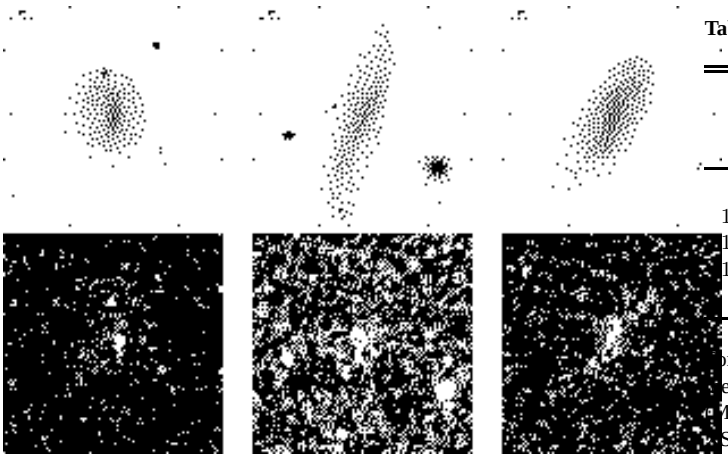

Figure 4. Examples of three bright ($r \leq 14.5$ mag) LSBs from MGSphot-only without matches in 2MASS. From left to right, the J2000.0 coordinates are (09:08:51.02,+03:26:54.0), (15:04:30.15,-00:51:04.8) and (12:11:19.92,+01:29:32.2). For each case, we show the colour image from SDSS (top) and the 2MASS K-band image from the same region of sky (bottom). These large, bright galaxies are too low-surface-brightness to be detected by the 2MASS pipeline. Images are $101''$ on a side, east is to the left, and a $10''$ line is given in the upper left of each optical image from SDSS.

matches brighter than $K = 13.57$ mag. Here we plot the CFs with variable binning such that the number of MGSphot+spec sources per parameter interval is constant. For comparison, we show the MGSphot+spec property distributions (grey histograms) for each r magnitude interval, and we tabulate the breakdown of galaxies within these bins in Table 2.

Table 2. Galaxy counts per r-magnitude interval.

Interval	Number				
	Total	XSC	XSC cut	PSC	Unmatche
$r \leq 15.0$	5012	4780	4777	124	108
$15.0 < r \leq 16.0$	16093	14864	14379	759	470
$16.0 < r \leq 17.0$	60807	45061	22567	11379	4367
$17.0 < r \leq 17.5$	74876	25037	1940	39454	10385
Totals	156788	89742	43663	51716	15330

r each extinction-corrected Petrosian r-magnitude interval (1), we give e total number of galaxies (2) from the MGS spectroscopic sample IGSphot+only) and the number of matches found in the XSC (3), the SC with a faint $K = 13.57$ mag cut (4), the PSC (5), and the remaining amount that have no matches in either the XSC or PSC (6). These magnitude intervals correspond to average XSC galaxy completeness values of 95.4, 92.4, 74.1, and 33.4 percent.

3.1 Conditions for Which the XSC is > 90 Percent Complete

At a magnitude cut of $r \leq 15$ (Fig. 6, second row of panels), 2MASS detects galaxies in the XSC at better than 95% completeness. The small fraction not detected in the XSC is from blue ($g - r < 0.5$), low concentration ($c_r < 2$) systems at low redshift ($z < 0.02$), split roughly between galaxies not in 2MASS at all (i.e., not in the XSC or PSC), and galaxies detected by 2MASS as point-sources. The nondetections have large angular sizes ($r_{50,r} > 10.''$) and, hence, low surface brightnesses ($\mu_{50,r} > 22$ mag/arcsec^2). The remaining galaxies missed by the XSC have high-surface-brightness ($\mu_{50,r} < 18.5$ mag/arcsec^2) and are detected in the PSC, yet with systematically elongated axis ratios ($\langle b/a \rangle_r < 0.3$). As expected, the galaxies in the PSC are unresolved by 2MASS with $r_{50,r} < 3''$; therefore, the trend towards

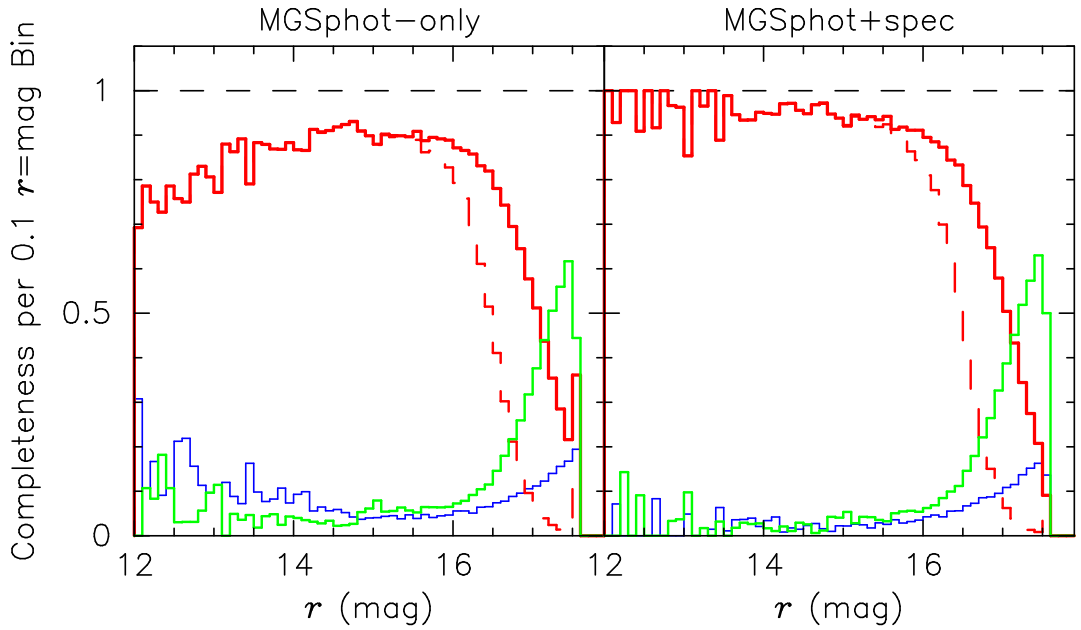

Figure 3. Completeness of subsamples relative to the MGSphot-only (left) and MGSphot+spec (right) primary samples as a function of extinction-corrected r-band magnitude. For each $\Delta r = 0.1$ mag bin, we plot the fraction of MGS sources with XSC (red), PSC (green), and no (blue) matches relative the normalised primary samples (horizontal dashed lines). We plot the $K \leq 13.57$ mag XSC matches as dashed red lines. In the left panel we note that the XSC appears to be badly incomplete at magnitudes brighter than $r = 15$. We stress that this is the result of contamination by bright image artifacts in the MGSphot-only, rather than actual bright sources missed by the XSC (see §2.4). The right panel shows the actual XSC completeness, which is $> 90\%$ for $r \leq 16$ mag.

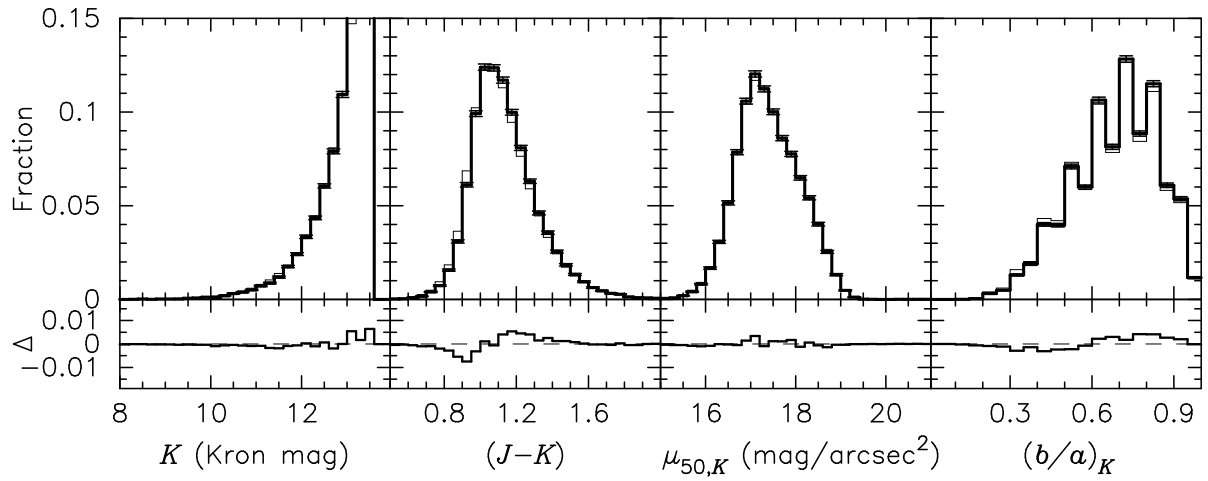

Figure 5. Comparison of two selections of 2MASS galaxies with $K \leq 13.57$ mag (97.5% completeness): (1) the 548,132 XSC objects outside of the Galactic plane ($|b| > 20°$) with galaxy-like colours of $0.1 \leq (J-K) \leq 2.5$ (thin line), and (2) the 43,663 XSC galaxies matched to the $r \leq 17.5$ DR2 spectroscopic sample (bold line). In each panel we compare the DR2 region and overall high-latitude relative distributions for four primary parameters: (from left to right) K-band Kron magnitude, $(J-K)$ colour, K-band mean surface brightness within $\mathrm{r}_{50,K}$, and K-band axis ratio. For each parameter, the difference (DR2−high-latitude) between the relative fractions is given at the bottom of each panel. We show the Poisson errors per bin for the 2MASS-SDSS matched subsample distributions, which are smaller typically than the per-bin differences. The subsample of $K_c \leq 13.57$ 2MASS galaxies with DR2 counterparts is representative of the full 2MASS XSC outside of the Galactic plane.

an over representation of $\langle b/a \rangle_r < 0.3$ galaxies in the PSC at all r magnitude intervals is the result of different spatial resolutions for SDSS ($1\farcs4$ median Abazajian et al. 2004) and 2MASS ($2-3''$) (Jarrett et al. 2003). At fainter r, the PSC axis ratio CFs are nearly flat, which means that galaxies detected by the PSC are not preferentially round, they are merely un-resolved. In general, apparently bright galaxies that 2MASS does not detect in the XSC are concentrated at the extremes of the property distributions observed at optical wavelengths. In other words, 2MASS detects $r \leq 15$ mag galaxies at 95.4broad range of normal optical properties.

We provide an alternative way to view the completeness of the XSC in Figure 7. In terms of absolute quantities, we show the r-band luminosity-size plane ($M_r - \mathrm{r}_{50,r}$; i.e., Petrosian absolute magnitude versus half-light radius) and we see that for $r \leq 15$ the 108 nondetections (blue circles) are intrinsically small and faint in visible red light. In contrast, we find that the 124 PSC-only detec-

tions (green triangles) occur throughout the same general envelope of absolute magnitude and size as the the nearly complete XSC sample shown by the red contours.

The XSC galaxy completeness remains $> 90\%$ per r mag bin, and 92.4average, for $15.0 < r \leq 16.0$ mag (third row in Fig. 6). The incompleteness continues to be dominated by nearby sources with $z < 0.04$, of which 60% are detected in the PSC. The rest are too low-surface-brightness to be detected by 2MASS in the XSC or PSC. The XSC is most complete for concentrated $c_r > 2.6$, red ($g - r > 0.6$) galaxies with $\mu_{50,r} < 21.5$ mag/arcsec^2. We note that for $r \leq 16.0$ mag, there is little difference in the completeness for all sources from the XSC, and the subset brighter than $K = 13.57$ mag (thin red lines). At the resolution limit of 2MASS, about half of the $\mathrm{r}_{50,r} < 2''$ MGS galaxies, some of which have red colours, are found in the PSC; and the rest have XSC detections. As seen at brighter r magnitudes, the known galaxies that altogether escape 2MASS detection tend to be blue LSBs with low concentration indices. As such, we see these galaxies are confined to a different part of the $M_r - \mathrm{r}_{50,r}$ plane than the bulk of normal galaxies detected by the XSC (see upper right panel of Fig. 7). This behaviour for the nondetections is precisely what is expected in a surface brightness-limited survey. We note that as with the brighter cases, the un-resolved galaxies found in the PSC continue to span the full range of M_r and intrinsic $\mathrm{r}_{50,r}$ populated by XSC matches (red contours).

We further investigate the low-level incompleteness at $r \leq 16$ mag with a visual inspection of the optical and near-IR image data at the precise location of MGS objects without XSC matches. First, we visually inspect all 232 (124 PSC, 108 unmatched) with $r \leq 15$ mag. We find that 42 (18%) in fact have XSC counterparts, but with 2MASS-SDSS coordinate offsets larger than the criteria we use for cross correlation (see Appendix A). We remind the reader that our assessment of the completeness characteristics of 2MASS galaxies depends on our statistically-derived criteria that assures negligible contamination from multiple and random matches. Another 27% (62) are false detections of bright galaxies by SDSS. We find 40 are either faint background galaxies that have falsely boosted flux as the result of overlap from the outer regions of a large foreground galaxy or a very bright and nearby star, or are part of a larger galaxy that was over deblended by the SDSS pipeline. In addition, 22 of the PSC matches are actual point sources (stars or compact nebulae). We display examples of each of these false detections in the top row of Figure 8. The rest of the objects that escape XSC detection are galaxies with visual characteristics in agreement with what we find from Figure 6. Namely, bright galaxies in the PSC have bright round nuclei and faint extended near-IR light that falls below the XSC detection, while all unmatched galaxies are late-type systems that are too low-surface-brightness to be adequately detected by 2MASS (see examples in the bottom two rows of Fig. 8). We note that $> 1/3$ of the PSC galaxies have close companions of roughly equal brightness. The companions are found in the XSC, thus, in these cases the 2MASS processing must have attributed the common halo of each pair to one galaxy (found in the XSC), and classified the second nucleus as a point source. These galaxies have early-type morphologies, and are possible "dry merger" candidates[6]. If we remove the 62 false SDSS detections and include the 42 XSC matches with large coordinate mismatches, we find an XSC completeness of 97.4% at $r \leq 15$ mag.

Next, we inspect the images for a random 25% sampling of the $15 < r \leq 16$ objects not found in the XSC (190 PSC, 117 unmatched). Even though our cross-correlation criteria in this magnitude range is more restrictive, the fraction of examples that have XSC counterparts outside of our criteria is now less than 8%. We find 79 (26%) with false SDSS galaxy detections, of which 62 are the result of point sources making it into the MGS. The remaining sources are LSBs (unmatched) and the bright cores of centrally-concentrated galaxies, with a 3-fold decrease in the number of close pairs. The bottom line here is that a complete visual inspection of over 1200 nonmatches could improve the already 92.4% overall XSC completeness at $15 < r \leq 16$ mag by a few percent.

3.2 Conditions for which the XSC Becomes Noticeably Incomplete

Between Petrosian r-band magnitudes of 16.0 and 17.0, the XSC galaxy completeness decreases rapidly from 90% to only 50%. As shown in the fourth row of Figure 6, we see many of the same trends as for brighter galaxies, i.e. 2MASS is most complete for more concentrated ($c_r > 2.6$) and redder ($g - r > 0.7$) galaxies with $\mu_{50,r} < 21$ mag/arcsec^2. In this r-magnitude interval, the differences in completeness when including all sources from the XSC, and the subset brighter than $K = 13.57$ mag (thin red lines), becomes apparent. As one would expect, a strict K-band magnitude cut omits galaxies that are intrinsically fainter and bluer, which are typically lower in concentration and surface brightness. The MGS sources not found in the 2MASS extended or point source catalogues concentrate towards the same extremes of optical parameter space as at bright fluxes, that is blue, low-concentration, low-surface-brightness, and low redshift.

For $16 < r \leq 17$ mag, 72% of the MGS sources missed by XSC are present in the PSC, yet a large fraction of these have r-band angular sizes that are big enough to be resolved by 2MASS. Near the 2MASS resolution limit, we find that nearly $3/4$ (8188) of the PSC-detected galaxies with $16 < r \leq 17$ have $\mathrm{r}_{50,r} > 2''$. This subset of larger PSC galaxies have median parameter values of $(g - r) = 0.58$, $c_r = 2.36$, and $\mu_{50,r} = 21.1$ mag/arcsec^2, which is suggestive of more late-type morphologies, and explains the changes in the behaviour of the parameter CFs compared with those at brighter r cuts. Indeed, a more conservative cut at $\mathrm{r}_{50,r} > 3''$, which is certainly resolved, still comprises 35% of the galaxies found in the PSC only. In other words, we are seeing the limit at which the disks and low-surface-brightness features of fainter late-type galaxies fall below the detection limit of the XSC algorithm, which in effect is primarily a cut in surface-brightness. To illustrate this point, in Figure 9 we show SDSS and 2MASS images of several random PSC examples with $\mathrm{r}_{50,r} > 3''$ and $16 < r \leq 17$ mag. With the greater depth and resolution of SDSS we see disk-dominated galaxies in the optical, but in the 2MASS images the brighter cores of these sources appear as small, concentrated objects and are point-like. At each successive r cut we probe

[6] Recent studies (van Dokkum et al. 1999; Bell et al. 2005) of $z > 0.5$ early-type galaxies have found small numbers of elliptical-elliptical galaxy mergers (so-called "dry" because of the assumed lack of cold gas), which are likely an important route for the formation of massive early-type galaxies.

larger redshifts on average, which results in more later-type galaxies falling below the detection limit of the XSC algorithm. This is confirmed by the $M_r - \mathrm{r}_{50,r}$ distribution of PSC detections (lower left of Fig. 7), where we see that the green contours tend toward somewhat lower surface brightness than the XSC galaxies; i.e., the PSC luminosity-size distribution is shifted in the direction of lower average luminosity relative to that of the XSC. The galaxies not found in 2MASS continue to populate the low-surface-brightness part of this parameter space, with increased numbers extending into the envelope defined by the XSC.

Finally, at the faintest half-magnitude interval of the complete SDSS spectroscopic selection of galaxies (bottom panels of Fig. 6; lower right of Fig. 7), we observe a continuation of the above trends for the $16 < r \leq 17$ interval. The surface brightness limit of the XSC selection, combined with the fainter brightness and greater redshift on average, extend the unmatched CFs further into each parameter distribution; therefore, we find that ever more concentrated, redder, and high-surface brightness galaxies are missed altogether by 2MASS. Moreover, more than half of the MGS has only a point-source detection in 2MASS in this r bin, with 51% (8%) of these having optical sizes of $\mathrm{r}_{50,r} > 2''$ ($> 3''$). Thus, most faint MGS galaxies in the PSC are semi-resolved at best. The PSC and XSC $M_r - \mathrm{r}_{50,r}$ relations are nearly identical, with a growing number of nondetections populating a similar luminosity-size space. The XSC is increasingly more complete for the most distant galaxies in the MGS, which is expected due to their typically redder colour.

4 NATURE OF GALAXIES DETECTED AND MISSED BY 2MASS

Now that we have quantified the detailed completeness of the 2MASS galaxy sample, we move on to discuss further the nature of galaxies both included in, and absent from, this K-band-selected sample. By nature we mean inherent qualities such as rest-frame luminosity, physical size, and colour. For this we use the suite of SDSS and 2MASS measurements, corrected to rest-frame $z = 0$, to study the optical and near-IR nature of galaxies in the XSC. Of particular interest is the character of galaxies that 2MASS misses, determined by quantifying the rest-frame properties of known galaxies found only as 2MASS point sources or completely lacking detection in 2MASS.

4.1 Optical Properties of Galaxies Outside of 2MASS Detection

Recall, the MGSphot+spec represents a representative sample of local galaxies that is magnitude ($r \leq 17.5$) and surface brightness ($\mu_{50,r} \leq 23.0$ mag/arcsec^2) limited. Comparison with the median values of each property distribution from the MGS (see Table 1) allows us to quantify which galaxies fall outside of 2MASS detection. For example, among these galaxies, 95% are less concentrated than the median ($c_r = 2.65$) MGS source. The SDSS concentration has been shown to correlate roughly with morphology (Shimasaku et al. 2001; Strateva et al. 2001), and a value of $c_r = 2.6$ is commonly used to separate early and late morphological types (Strateva et al. 2001; Kauffmann et al. 2003; Bell et al. 2003a,b). This value is very close to the MGS median; therefore, the galaxies missed by 2MASS are systematically late type. As we demonstrated in §3, the average galaxy that escapes 2MASS detection is much bluer and lower-surface brightness than the typical MGS galaxy, fully consistent with late-type morphologies. Indeed,

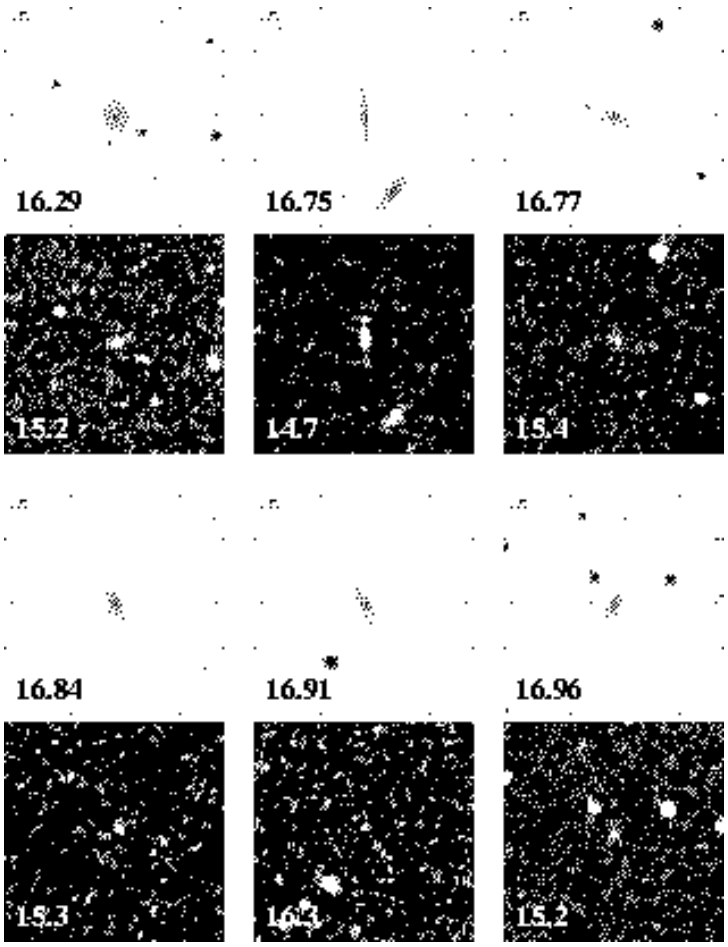

Figure 9. Examples of $16 < r \leq 17$ mag MGS galaxies with $\mathrm{r}_{50,r} > 3''$ that are detected as point sources by 2MASS. As in Figure 8, we display the optical and K-band images for each example, and give the r and K brightnesses. Only the centres of faint disk-dominated galaxies in SDSS are detected by 2MASS, which explains why they appear in the PSC.

even at optically bright magnitudes, these systems are visually very late-type spirals, LSBs, or irregulars (see bottom row of Fig. 8).

As noted by Strauss et al. (2002), the SDSS half-light sizes are not corrected for seeing, which biases concentration values downwards for galaxies with sizes comparable to the PSF size (typically $1\farcs4$). The galaxies missed by 2MASS are larger on the sky with a median size of $3.55''$ compared to the MGS median size of $2.46''$; therefore, we are confident that the low-concentration nature of the missed systems are not affected by seeing. Furthermore, this difference in apparent size highlights why 2MASS preferentially misses these galaxies. At a given r magnitude, the unmatched galaxies have the largest angular sizes, which translates into the lowest apparent surface brightnesses. This is exactly the behaviour one expects from a shallower magnitude-limited survey. Moreover, the median redshift difference of $z_{\mathrm{med}} = 0.057$ for nondetections, compared to $z_{\mathrm{med}} = 0.092$ for $r \leq 17.5$ mag galaxies from SDSS, owes to this surface brightness selection effect. This selection effect begins at $\mu_{50,r} \approx 21.5$ mag/arcsec^2 (see Fig. 6), or 1.5 mag brighter than the MGS limit. Even at bright optical magnitudes where the XSC is $> 90\%$ complete, a fraction of the largest ($\mathrm{r}_{50,r} > 5''$) galaxies are not detected. We see from Figure 10 that the XSC detects galaxies larger than $5''$ but limited in mean surface brightness to $\mu_{50,K} \leq 19.5$ mag/arcsec^2, which is 0.5 (1) mag

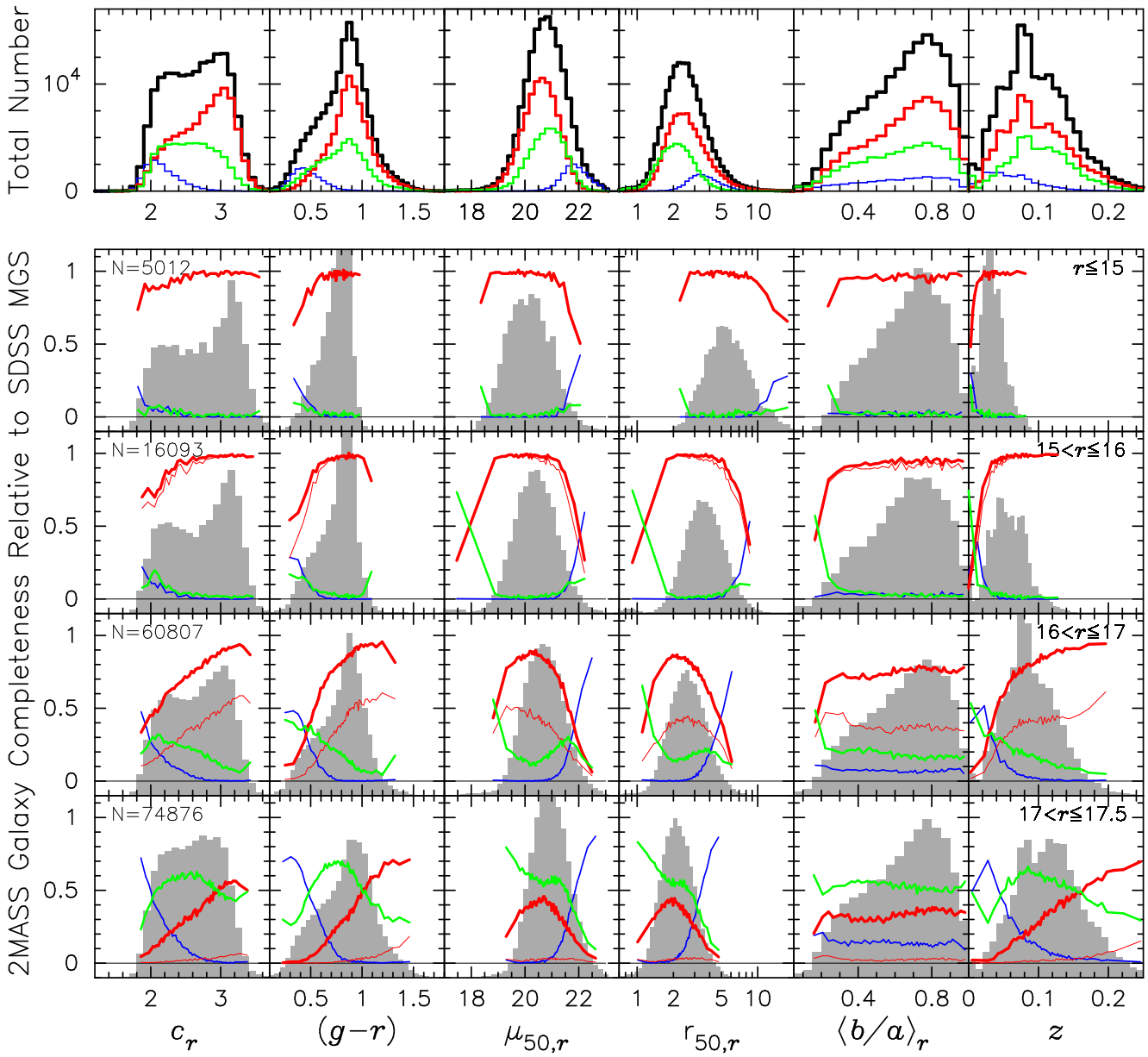

Figure 6. *Top row*: Observed optical property distributions for the SDSS "main" spectroscopic galaxy selection (MGSphot+spec; see text for details) limited to have extinction-corrected Petrosian magnitudes brighter than $r = 17.5$. Shown from left to right are r-band concentration given by $c_r = \mathrm{r}_{90,r}/\mathrm{r}_{50,r}$, $(g-r)$ model colour, half-light r-band surface brightness in mag/arcsec^2, Petrosian half-light radius in arcseconds (r-band), average r-band axis ratio b/a (see §2.3), and spectroscopic redshift z. In each panel, we plot the total sample (black) of 156,788 galaxies with photometric and spectroscopic properties from DR2, and the subsamples from our cross correlation with the 2MASS XSC (thick red, $N = 89,742$) and PSC (green, $N = 51,716$). In addition, we show the subsample of 15,330 galaxies without 2MASS counterparts (blue). *Lower panels*: Completeness of 2MASS galaxies with respect to the SDSS spectroscopic sample (MGSphot+spec) as a function of six fundamental parameters. The completeness functions (CF, see text for details) are given for four different r magnitude cuts corresponding to 95%, 90%, 50%, and 10% minimum XSC completenesses per interval (see Fig. 3). We indicate the total number of galaxies per bin in the left-most panel. The thin red line shows the $K \leq 13.57$ magnitude-limited XSC sample, which contains a total of 43,663 galaxies. A thin black line marks zero completeness in each panel, and for each magnitude interval we plot the MGSphot+spec property distributions in relative counts (grey histograms).

brighter (fainter) than the 1σ (3σ) background noise in 2MASS K-band images (Jarrett et al. 2000). Therefore, we qualify the statement by Jarrett et al. (2003) that galaxies larger than $10 - 15''$ in diameter, but less than $50''$, are fully sampled in the XSC *if* their K-band surface brightness averaged over the half-light diameter is 0.5 mag above the 2MASS background. We note that the most low-surface-brightness galaxies in the 2MASS Large Galaxy Atlas are within this limit.

Finally, in Figure 11 we further demonstrate the different nature of MGS galaxies not detected by 2MASS. Relative to the statistically-complete MGS (shown in black), the galaxies missed by 2MASS (blue histogram) are significantly lower in luminosity and bluer, yet they have similar physical size distribution. There-

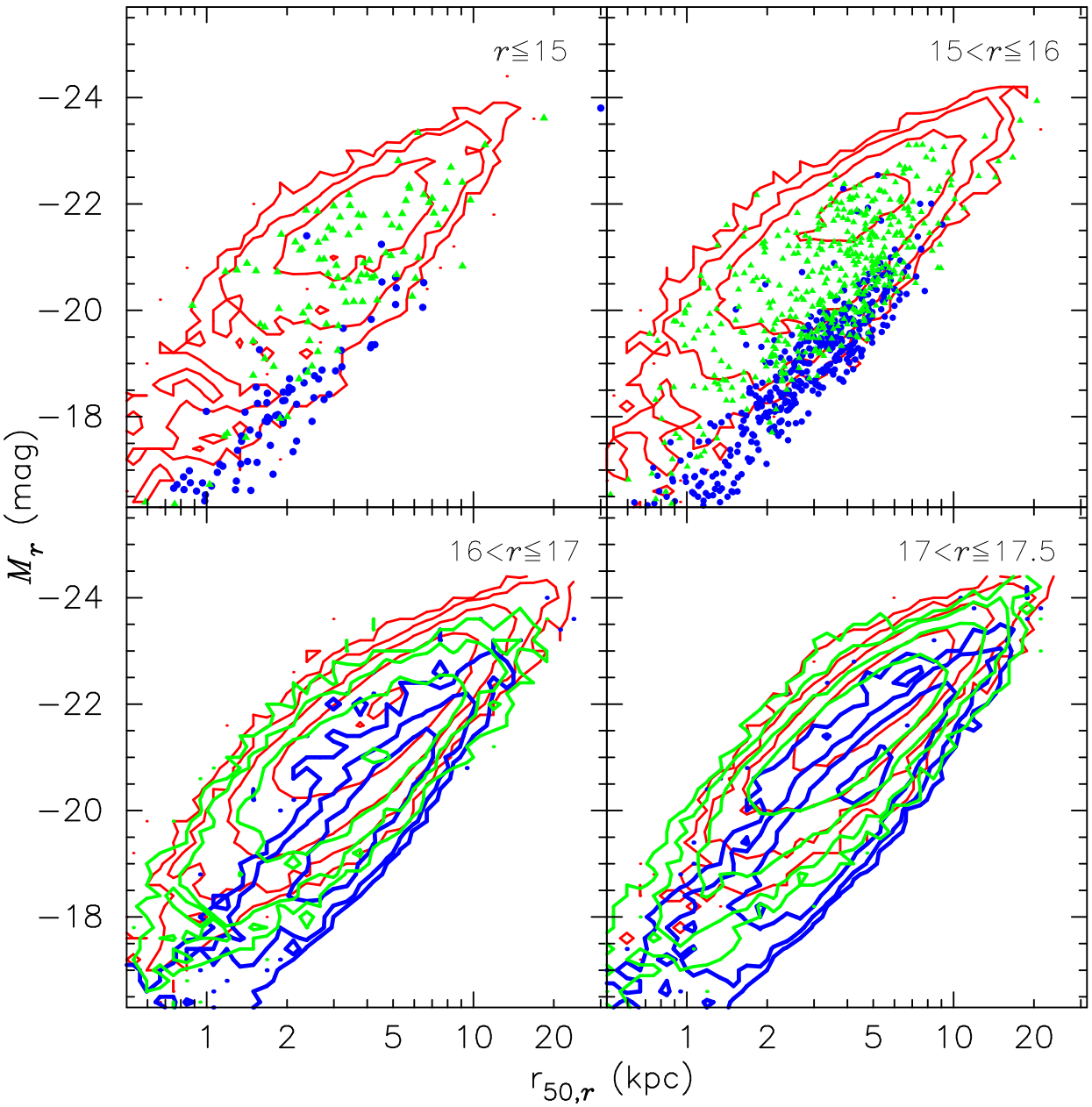

Figure 7. Petrosian r-band luminosity-size ($M_r - \mathrm{r}_{50,r}$) planes for four r magnitude intervals defined by minimum XSC completeness values per bin of 95%, 90%, 50%, and 10% (see text for details). In each panel we plot the absolute r-band magnitude against the intrinsic half-light size in kiloparsecs. As in Fig. 6, red denotes galaxies from the XSC, green the PSC, and blue represents nondetections in 2MASS. Contours show levels of constant number density in powers of three: 1, 3, 27, 81, 243, and 729.

fore, the differences in angular size between nondetections and all MGS galaxies are primarily the result of their *intrinsic* low surface brightness, i.e. at a given physical size, galaxies missed by 2MASS have lower luminosity than typical galaxies detected by 2MASS.

4.2 Optical Properties of Faint Galaxies in the PSC

A large fraction (33%) of MGS galaxies have 2MASS counterparts in the PSC only; 98% of these are fainter than $r = 16$ mag (see Table 2). Galaxies have PSC-only detections mainly because they are unresolved by 2MASS, with 44% (85%) having $\mathrm{r}_{50,r} \leq 2''$ ($3''$). The remainder have larger angular sizes, but their surface-brightness profiles fall below the 2MASS extended-source sensitivity and, thus, only their round and concentrated nuclei are detected. As we show in the middle row of Figure 8, even at bright total r magnitudes the outer portions of these galaxies are faint in the optical, and nearly invisible in near-IR light. In terms of morphology, the bright PSC detections that are large enough to be resolved by 2MASS are either disk-dominated systems with low-surface-brightness disks, or early-type galaxies in close pairs. At fainter than $r = 16$, these galaxies appear to be mostly disk-dominated (see Fig. 9). We conclude that the late-type galaxies with higher-surface brightness disks and large enough angular sizes to be resolved by 2MASS are detected readily in the XSC at $r \leq 16$, while

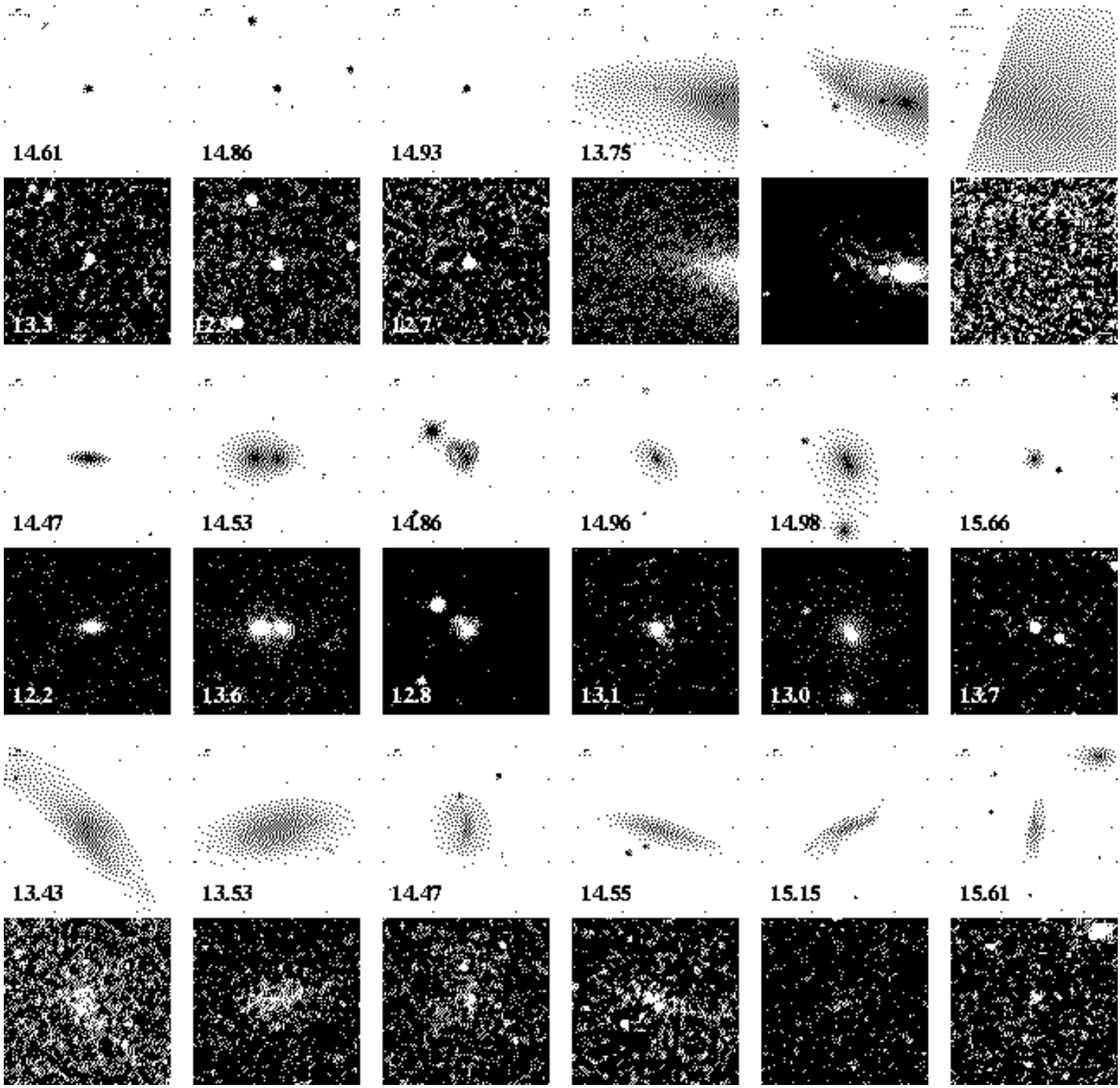

Figure 8. Examples of $r \leq 16$ mag MGS objects that are not detected in the XSC. For each row, we display the SDSS optical (top) and 2MASS K-band (bottom) images. We also show the extinction-corrected Petrosian r magnitudes and, for sources from the PSC, we indicate the default aperture magnitude K, which is a rough measure of the total galaxy light. Top row: the first three panels show sources with PSC matches that appear to be point-like (actual stars or unresolved nebulae), and the last three panels give examples where SDSS falsely detects a bright galaxy as the result of overlap from a large foreground galaxy, overdeblending of a large galaxy, and scattered light from nearby bright star. Second row: PSC-detected galaxies with bright round centres and low-surface-brightness extended features; among these we show examples with nearby bright companions from the XSC. Last row: typical examples of late-type galaxies with low surface brightnesses that are below 2MASS detection. Images are $101''$ on a side, east is to the left, and a $10''$ line is given in the upper left of each optical image from SDSS.

at fainter magnitudes their disks fall systematically below detection.

For determining the morphological nature of PSC-selected galaxies with $r_{50,r} \leq 3''$, their small angular sizes rule out comparisons with the seeing-dependent concentration parameter from the overall sample. Therefore, we turn to apparent $(g-r)$ model colour as a possible type discriminator. All galaxies in the PSC have a median and r.m.s. colour of $(g-r) = 0.81 \pm 0.25$, which is well-matched to values for the MGS ($g-r = 0.84 \pm 0.25$; see Table 1). Yet, we find the resolved and unresolved PSC galaxies have different median colours. The former are moderately blue ($g-r = 0.61$) as expected for later-type morphologies, while galaxies that are too small to be resolved by 2MASS have $(g-r) = 0.80$, which is close to the median colour of MGS galaxies, suggesting a range of galaxy types.

In terms of rest-frame properties, we see in Figure 11 that the PSC detections (in green) span similar relative distributions of optical luminosity, size, and $(g-r)_0$ colour (corrected to $z = 0$) as galaxies in the complete MGS (black). We notice a slight bias such that the total PSC sample is somewhat bluer, less-luminous, and smaller, but this shift is explained by the small fraction (15%) of resolved galaxies with late-type morphologies and low-surface-brightness disks that made it into the PSC. The relative differences between the MGS and its PSC subsample are minor for each property; therefore, we surmise that truly unresolved galaxies detected by the PSC span the full range of colours, luminosities, physical sizes, and presumably types, as normal galaxies. So it is simply the larger cosmological distances ($z_{\rm med} = 0.102$) that explain the smaller angular sizes and typically fainter galaxy content of the PSC.

4.3 Optical and Near-IR Nature of Galaxies in the XSC

We combine near-IR galaxy parameters from 2MASS with the SDSS optical properties to describe the nature of 2MASS-selected galaxies. We find that 57% of $r \leq 17.5$ galaxies from the MGS spectroscopic sample have a match in the XSC, with the vast majority of nonmatches fainter than $r = 16$ mag. In Figure 11, we see small differences between the relative distributions of all MGS galaxies and the subset matched to the XSC (shown in red). The XSC covers a very similar range in physical sizes, but we see a shift towards more high-luminosity and redder galaxies because the nondetections tend to be intrinsically fainter and bluer as described in §4.1.

In Figure 10, we plot the observed 2MASS parameter distributions for MGS galaxies with XSC detections, split into four r magnitude bins that represent decreasing XSC completeness with decreasing brightness. We see that these galaxies span a broad range of apparent near-IR properties. For optically bright galaxies ($r \leq 16$ mag), the XSC is very complete with nearly all sources having $K \leq 13.57$ mag (black histograms). At $r > 16$ mag, many galaxies remain detected in the XSC, but with a growing number that have $K > 13.57$ mag, which is the limit where 2MASS becomes nonuniform and $< 97.5\%$ complete. For $16 < r \leq 17$ mag, roughly half of the XSC sources are fainter than $K = 13.57$ mag, while at $r > 17$ mag it is 92%. Naturally, this correspondence between optical and near-IR faintness leads to the decreasing completeness of the XSC at $r > 16$ mag as we show in Figure 3. Therefore, one must take care when defining galaxy samples from cross-correlated 2MASS and SDSS observations.

For example, selecting all galaxies with $r \leq 17.5$ and $K \leq 13.57$ will provide a magnitude-limited sample that is 97.5% complete within the K-band limit, but includes $r > 16$ galaxies that are preferentially red and concentrated (see Fig. 6). This colour preference is also seen in the apparent $(J-K)$ and $(r-K)$ distributions of $r > 16$ galaxies in the bottom two rows of Figure 10 (black filled histograms). Here the K-band magnitude-limited XSC contains 62% that is redder than the median apparent $(g-r)$ colour of the MGS. Clearly, the correlation between larger average redshifts for fainter r intervals produces overall shifts in the not-k-corrected $(J-K)$ and $(r-K)$ colours towards the red, which is likewise seen in the $(g-r)$ model colour distributions of Figure 6. Nevertheless, we have demonstrated in §3.2 that the XSC preferentially selects from the red side of the galaxy distribution at $r > 16$ mag. In Figure 12, we show examples of galaxies selected at random from the region of colour space ($1.0 < g-r \leq 1.2$) corresponding to the most complete XSC galaxies at $16 < r \leq 17$ mag. These faint galaxies with 2MASS detections are 90% bulge-dominated, consistent with their red colours.

Based on our analysis, selecting an XSC-MGS matched catalogue that is magnitude-limited to $K \leq 13.57$ and $r \leq 16$ produces the most representative sample with good statistical completeness (90.8%) and statistically useful numbers (19,156 for DR2; hereafter, we call this sample XSC_A). The near-IR cut ensures 97.5% completeness of K-band galaxies in the XSC, and the r-band cut provides 93.1% completeness in terms of MGS sources detected by the XSC. The top two rows of Figure 10 illustrate clearly that the XSC_A is representative of the full range of near-IR parameter space, and we have shown in §3.1 that these galaxies are quite representative in terms of observed optical properties. For reference, we show examples of blue ($0.6 < g-r \leq 0.7$) and red ($0.9 < g-r \leq 1.0$) galaxies from the XSC with $r \leq 16$ mag in Figures 13 and 14. We choose these colour cuts on either side of the median MGS colour such that the XSC selection is $> 95\%$ complete for sources within this range of colours. Approximately 90% of the blue galaxies are disk-dominated, the majority with obvious spiral features, while the red galaxies have early-type (bulge-dominated) morphologies. These figures demonstrate the normal nature of galaxies detected with 93.1% completeness in 2MASS.

We compare the intrinsic nature (luminosity, size, colour) of XSC_A with two other samples based on the XSC-MGS cross correlation: the $r \leq 17.5$ MGS matched to the XSC (XSC_B), and the subset limited in K-band to brighter than 13.57 mag (XSC_C). Using the DR2-derived MGS, XSC_B and XSC_C contain 89742 and 43663 galaxies, respectively. We plot the relative property distributions at near-IR wavelengths in Figure 15, and at optical in Figure 16. Not surprisingly, applying a strict r magnitude cut to a K-band-limited sample (XSC_B $\rightarrow$ XSC_A) results in an additional blue-colour selection, which is well-illustrated by the $(J-K)_0$ differences in the right panel of Figure 15. Furthermore, the $r = 16$ mag limit restricts the volume of space from which these samples are drawn. Therefore, the XSC_A sample contains fewer luminous ($M_K < -24.5$ and $M_r < -22.0$) and large (> 4 kpc) galaxies compared to the XSC_B and XSC_C. The smaller median redshift of XSC_A ($z_{\rm med} = 0.052$) compared to the XSC_B (0.115) and XSC_C (0.093) confirms these trends.

5 CONCLUSIONS

In this paper we have addressed the basic question: What is the nature of galaxies detected and missed by 2MASS? We have matched 2MASS extended and point sources to the spectroscopically-confirmed sample of over 155,000 bright ($r \leq 17.5$ mag) galaxies

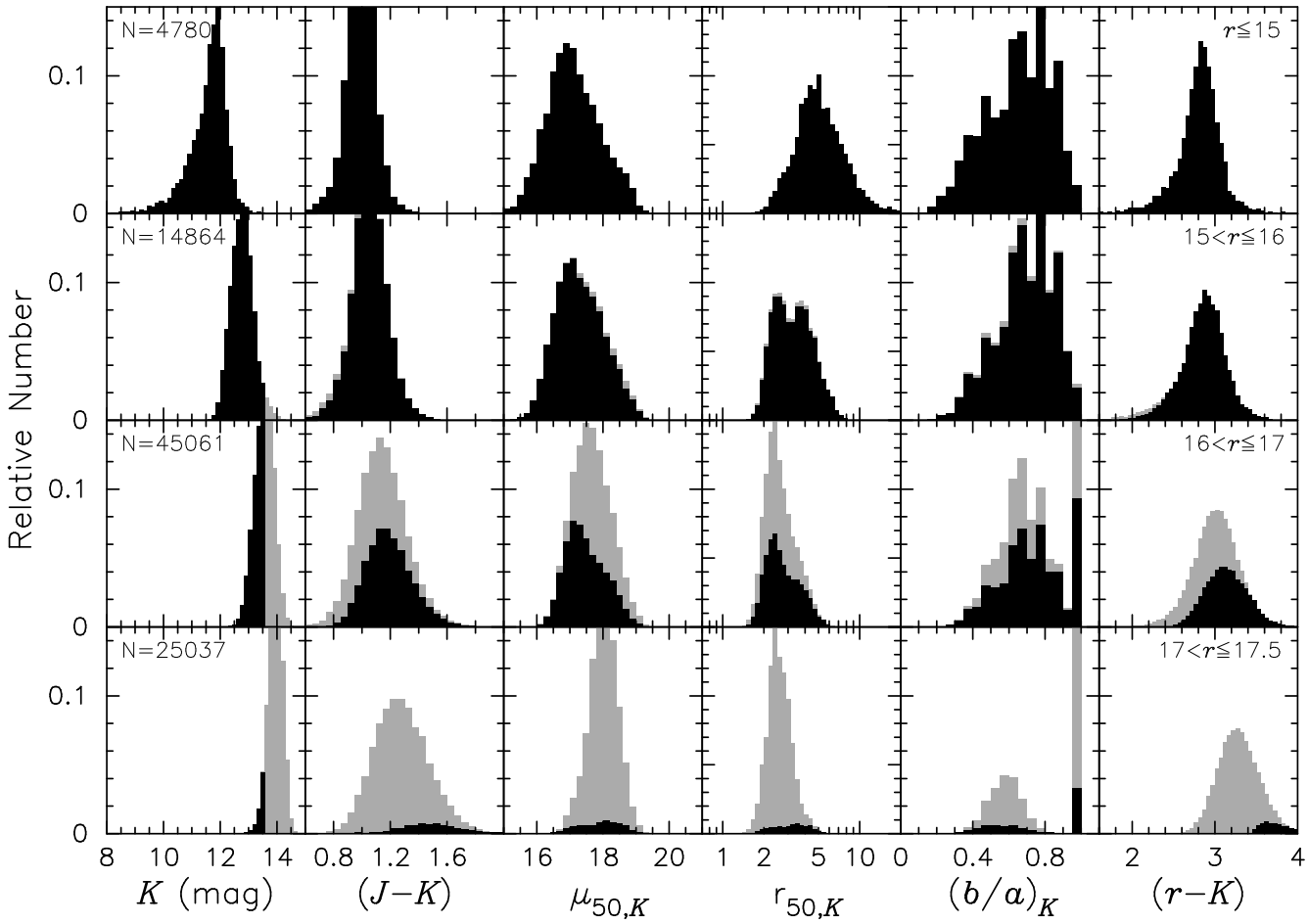

Figure 10. Near-infrared-derived property distributions from the XSC for 2MASS galaxies in the SDSS spectroscopic sample (MGSphot+spec) split into four different r magnitude intervals corresponding to 95%, 90%, 50%, and 10% minimum XSC completenesses per bin. From left to right we give the apparent K-band Kron magnitude, $(J-K)$ colour, average half-light surface brightness $\mu_{50,K}$, circularised half-light radius $\mathrm{r}_{50,K}$, axis ratio $(b/a)_K$, and Petrosian r minus Kron K colour. We give the total distributions in grey and the $K \leq 13.57$ mag cut in black. For each r mag bin, we give the total number of XSC galaxies in the left-most panel.

from the SDSS (MGS). We assume that the MGS provides a globally representative sample of local galaxies with which to quantify the average optical properties of galaxies that 2MASS does and does not detect. From the cross correlation with MGS we find that 2MASS detects 90% of SDSS galaxies brighter than $r = 17$ mag. We find that naively applying the MGS criteria to a photometric-only selection from SDSS produces a less reliable set of galaxies with a $10-20\%$ contamination by image artifacts in the SDSS at $r < 15$ mag.

The 2MASS Extended Source Catalog (XSC) detects 93.1% of all galaxies in the spectroscopic MGS down to $r = 16$ mag. If one does a careful job of matching to MGS and weeding out spurious SDSS sources, a completeness of 97.5% can be achieved at $r \leq 15$ mag, with the only major source of incompleteness being blue LSBs. We have quantified the completeness in terms of fundamental optical properties from SDSS – concentration, colour, mean surface brightness, half-light radius, axis ratio, and redshift. We find that the bright galaxies in the XSC span the full range of optical properties exhibited by the SDSS main sample. The XSC selection of known galaxies suffers two primary systematics: (1) it is limited at the low-surface-brightness end as expected in a magnitude-limited selection; and (2) it has a spatial resolution limit of $2-3''$, which results in galaxies with smaller angular sizes being selected and placed in the 2MASS Point Source Catalog (PSC). The latter effect occurs mainly for galaxies fainter than $r = 16$ mag, which tend to be further away and, hence, smaller in angular extent. Fewer than 3% of $r \leq 16$ galaxies from the MGS escape 2MASS detection because they have low-surface-brightness and late morphological type (e.g., Sc-Sd spirals, irregulars). Another 4% are detected only by the PSC as a result of their bright round centres and faint outer profiles. Therefore, we conclude that the low-level incompleteness in the XSC at the bright end is caused by surface brightness selection effects.

At $16 < r \leq 17$, where the MGS remains highly complete, 2MASS continues to detect galaxies at 90% down to $r = 17$ mag but with increasing proportion in the PSC only. The majority (85%) of faint PSC detections are unresolved ($< 3''$) by 2MASS, with a broad range of normal properties and redshifts towards the more-distant tail of the distribution. As a result of the surface brightness-dependent selection effects, 15% of faint PSC galaxies are resolved disk-dominated systems with disks too faint to detect in 2MASS. Finally, 2MASS still finds more than 80% of the MGS fainter than $r = 17$ mag, with more than half in the PSC and only the most distant, red, and presumably early-type galaxies found in the XSC.

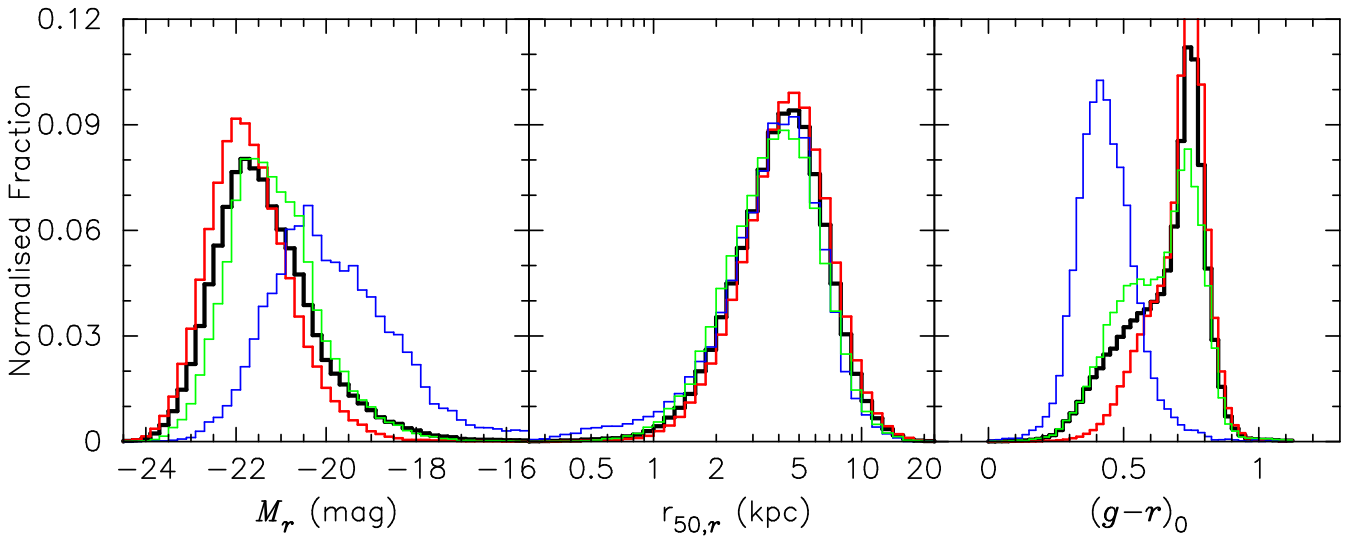

Figure 11. Normalised distributions of various 2MASS-related selections of subsamples from the MGS ($r \leq 17.5$ mag), in terms of rest-frame optical properties: absolute r-band magnitude (left), physical half-light radius in the r-band (middle), and rest-frame $(g-r)_0$ model colour (right). The magnitudes and colours are k-corrected to $z = 0$. In each panel, we compare the overall distribution from the MGS (black) with distributions from those galaxies in the XSC (red), in the PSC (green), and not detected by 2MASS (blue). We truncate the XSC normalised $(g-r)_0$ distribution slightly at redder colours so that we can resolve differences with other distributions at bluer colours.

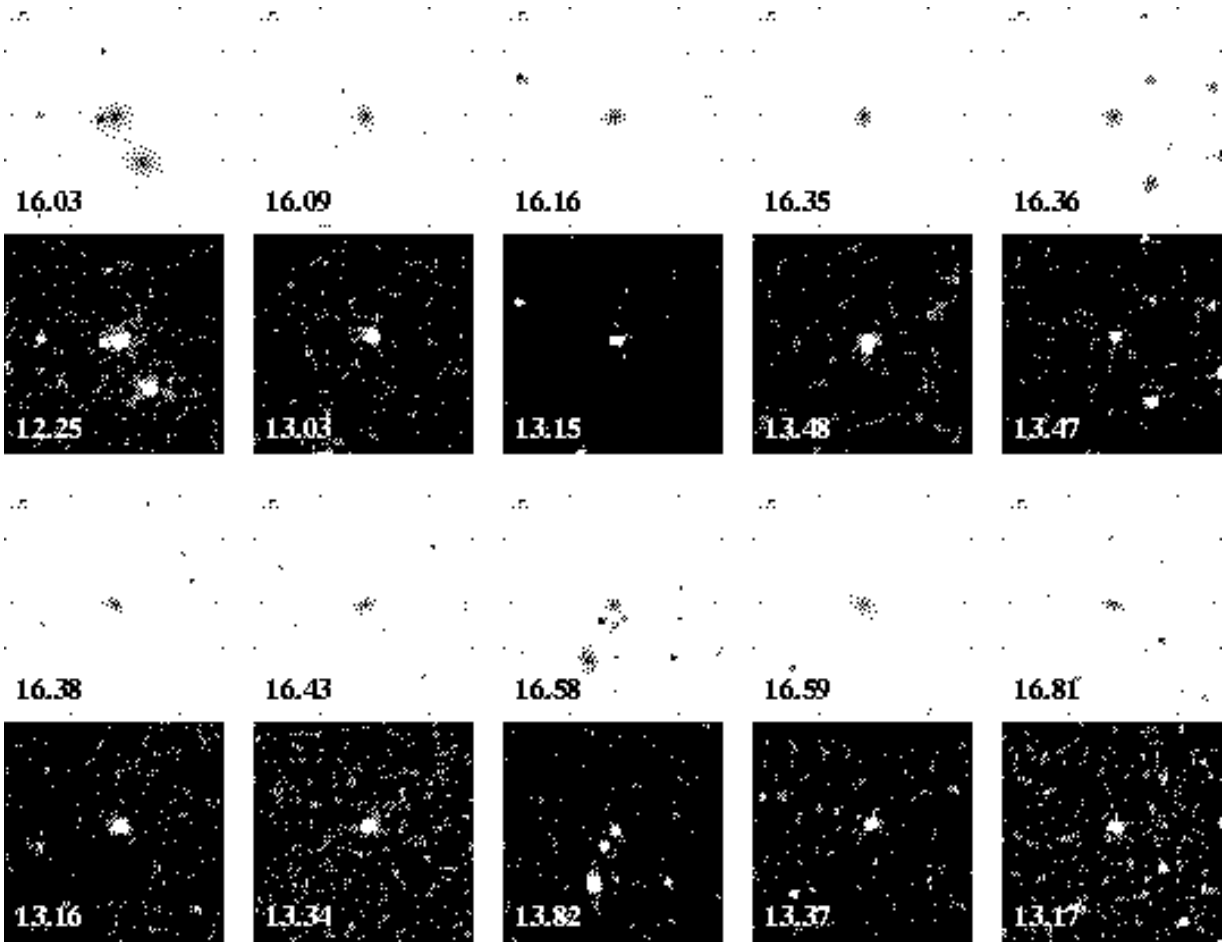

Figure 12. Examples of XSC galaxies with $16 < r \leq 17$ and red colours ($1.0 < g - r \leq 1.2$). Following the format of Figures 4, 8 and 9, we show $101 \times 101''$ optical and K-band images for each case. Here we indicate the Petrosian r and Kron K magnitudes. The galaxies are shown in decreasing r brightness from left to right. As illustrated here, galaxies meeting these criteria are bulge-dominated 90% of the time.

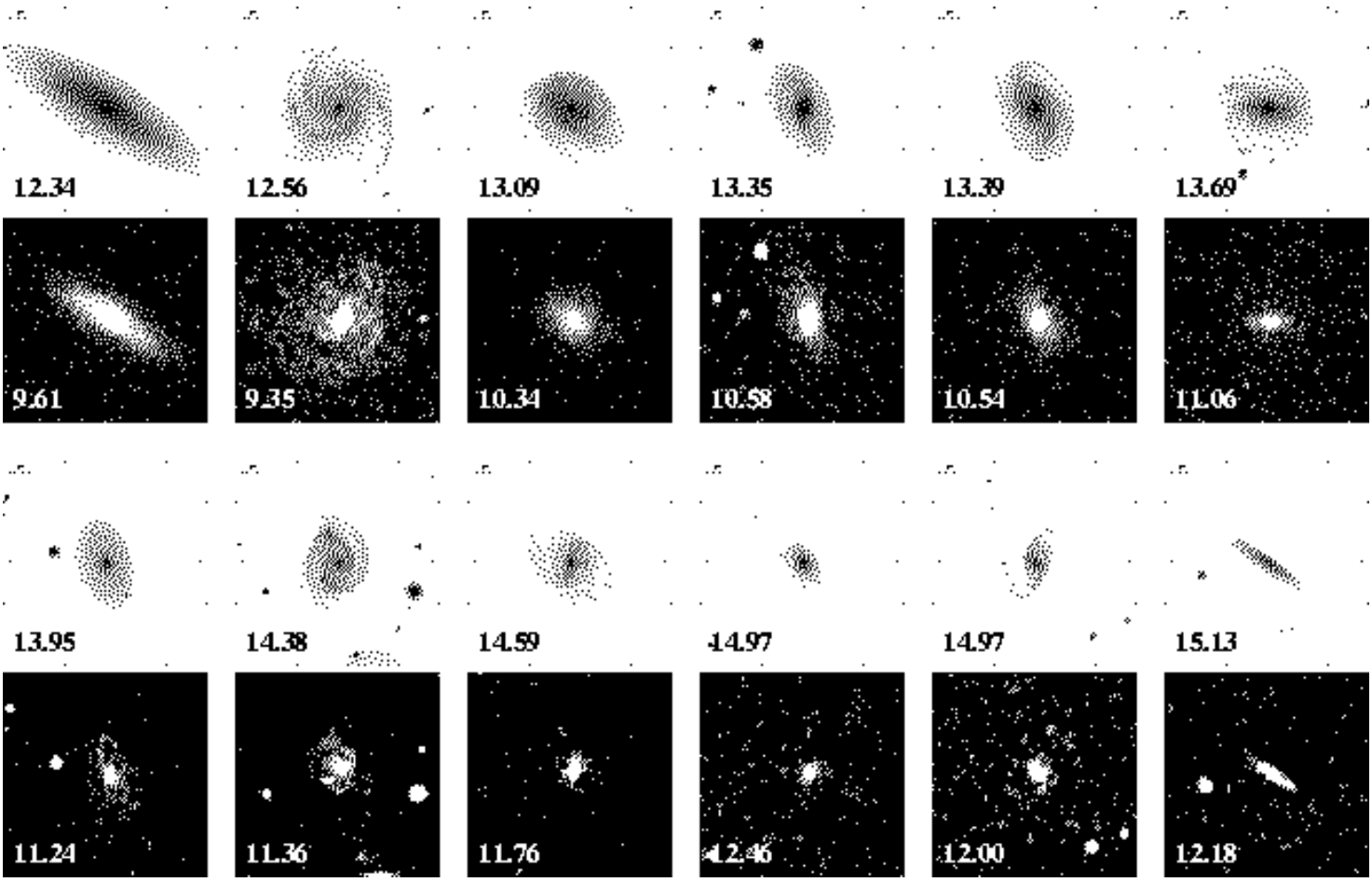

Figure 13. Examples of bright ($r \leq 16$ mag) blue ($0.6 < g - r \leq 0.7$) galaxies found in the XSC. We display the images as in Figure 12. Roughly 90% of galaxies with these r and $(g - r)$ criteria are disk-dominated, and nearly $2/3$ of these have obvious spiral structure in the SDSS images. We provide examples in these relative frequencies.

Because of the different selection effects of 2MASS and SDSS, one must be careful when defining samples of XSC-MGS matched galaxies based on statistically-complete magnitude cuts from each individual survey. For example, selecting all MGS galaxies with XSC matches will produce a sample that is incomplete at $r > 16$ mag and over-representative of red early-type galaxies. Likewise, all $K \leq 13.57$ galaxies from the XSC are complete in a K-magnitude sense, but preferentially miss blue and lower-surface brightness disk-dominated galaxies at $r > 16$ mag. We note that all MGS galaxies brighter than $K = 13.57$ are fully representative of the half million galaxies of similar brightness in the local universe as seen by 2MASS. This means that 2MASS *does not* find some special type of galaxy not present in the SDSS spectroscopic selection. Finally, we find that a combined $K \leq 13.57$ and $r \leq 16$ cut produces the most representative sample. Based on the DR2 version of the MGS selection, this sample contains 19,156 galaxies with 90.8% completeness, spectroscopic redshifts, and a suite of near-IR and optical properties.

ACKNOWLEDGEMENTS

We are very grateful to Rae Stiening, who has tirelessly maintained the *Two Micron All Sky Survey* (2MASS) catalogues and image data at the University of Massachusetts, and who has helped write efficient algorithms for searching the data base. We thank Roc Cutri, Tom Jarrett, and Steve Schneider for help with 2MASS. We are grateful for enlightening correspondence with Sloan team members Jennifer Adelman, Michael Blanton, Sebastian Jester, Huan Lin, Michael Strauss, and Douglas Tucker. Additionally, the authors appreciate useful discussions with Rose Finn, Kelly Holley-Bockelmann, and Ariyeh Maller. D. H. M. M. D. W. and N. K. acknowledge support from the National Aeronautics and Space Administration (NASA) under LTSA Grant NAG5-13102 issued through the Office of Space Science. M. D. W. and N. K. acknowledge support by NSF grants AST-9988146 & AST-0205969 and by the NASA ATP grant NAG5-12038. E. F. B. was supported by the European Community's Human Potential Program under contract HPRN-CT-2002-00316 (SISCO). This publication makes use of data products from 2MASS and the *Sloan Digital Sky Survey* (SDSS). 2MASS is a joint project of the University of Massachusetts and the Infrared Processing and Analysis Center/California Institute of Technology, funded by the National Aeronautics and Space Administration and the National Science Foundation. The 2MASS Web site is http://pegasus.astro.umass.edu/. We obtained SDSS data from the SDSS Catalog Archive Server (http://casjobs.sdss.org/casjobs/), and colour images presented here were downloaded with the SkyServer Image List Tool

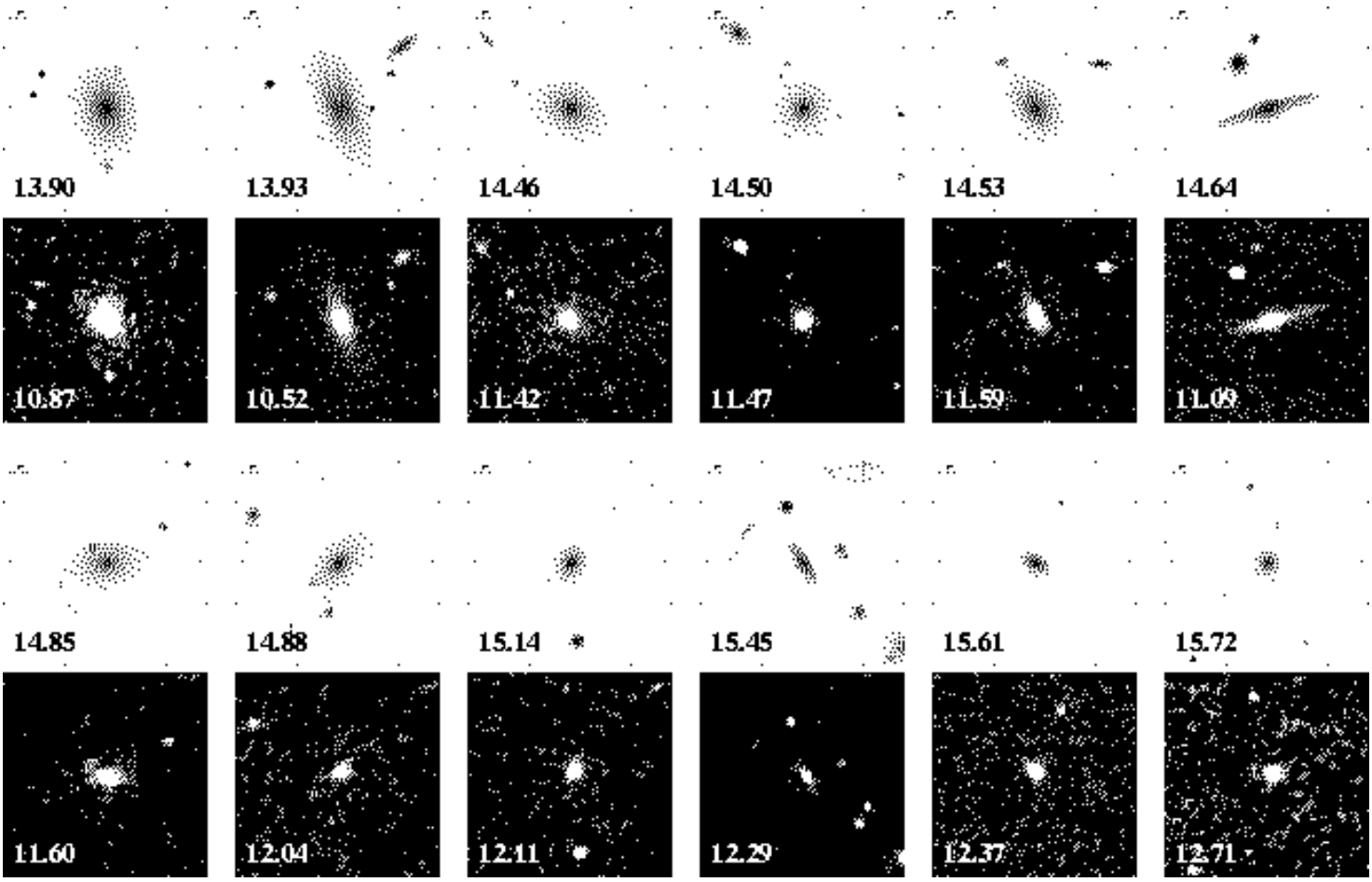

Figure 14. Same as in Figures 12 and 13, here we show examples of bright ($r \leq 16$ mag) red ($0.9 < g - r \leq 1.0$) galaxies with counterparts in the XSC. These galaxies have bulge-dominated and disk-dominated frequencies of 85% and 15%, respectively, as shown here.

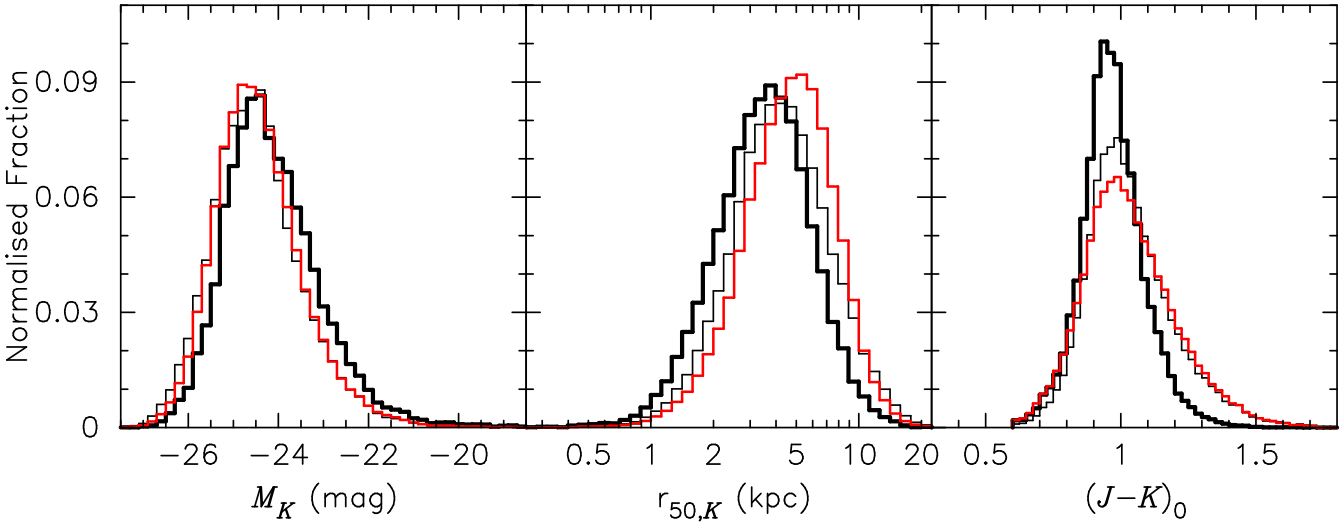

Figure 15. Relative normalised distributions of different K-magnitude cuts to the XSC-MGS matched sample in terms of rest-frame near-IR properties: absolute K-band magnitude (left), physical half-light radius in K-band (middle), and $(J-K)_0$ colour (right). The magnitudes and colours are k-corrected to $z = 0$. In each panel, we compare the distribution from all XSC-MGS galaxies (red; XSC_C) with distributions from subsets cut at $K \leq 13.57$ mag (thin black; XSC_B), and the most complete sample limited at both $K \leq 13.57$ and $r \leq 16$ mag (thick black; XSC_A).

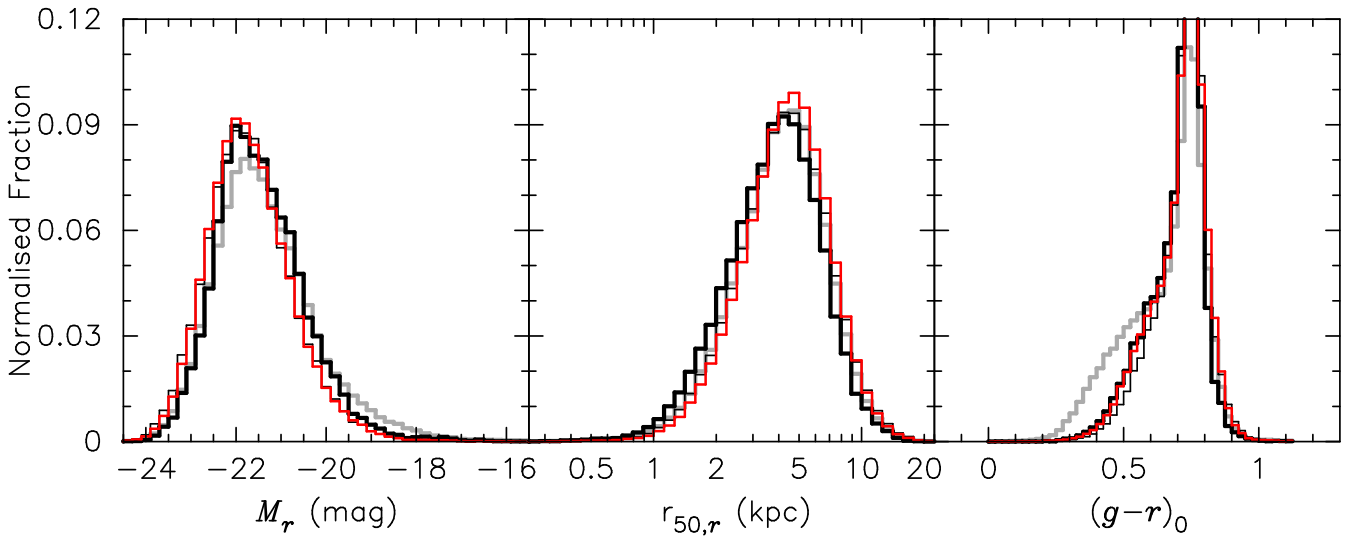

Figure 16. Relative normalised distributions of rest-frame optical properties as in Figure 11, but here for the different K-magnitude cut subsamples of the XSC-MGS matches as in Figure 15: XSC_A (thick black), XSC_B (thin black), and XSC_C (red). We include the overall distribution from the MGS in grey for reference. We truncate the XSC_C normalised $(g-r)_0$ distribution slightly at redder colours so that we can resolve differences with other distributions at bluer colours.

(http://cas.sdss.org/astro/en/tools/chart/list.asp). Funding for the creation and distribution of the SDSS Archive has been provided by the Alfred P. Sloan Foundation, the Participating Institutions, the National Aeronautics and Space Administration, the National Science Foundation, the U.S. Department of Energy, the Japanese Monbukagakusho, and the Max Planck Society. The SDSS Web site is http://www.sdss.org/. The SDSS is managed by the Astrophysical Research Consortium (ARC) for the Participating Institutions, which are the University of Chicago, Fermilab, the Institute for Advanced Study, the Japan Participation Group, the Johns Hopkins University, Los Alamos National Laboratory, the Max-Planck-Institute for Astronomy (MPIA), the Max-Planck-Institute for Astrophysics (MPA), New Mexico State University, University of Pittsburgh, Princeton University, the United States Naval Observatory, and the University of Washington. This publication also made use of NASA's Astrophysics Data System Bibliographic Services.

REFERENCES

Abazajian K., Adelman-McCarthy J. K., Agüeros M. A., Allam S. S., Anderson K. S. J., Anderson S. F., Annis J., Bahcall N. A., Baldry I. K., Bastian S., et al. 2003, AJ, 126, 2081

Abazajian K., Adelman-McCarthy J. K., Agüeros M. A., Allam S. S., Anderson K. S. J., Anderson S. F., Annis J., Bahcall N. A., Baldry I. K., Bastian S., et al. 2004, AJ, 128, 502

Adelman-McCarthy J. K., et al. 2005, ApJ submitted, (astro-ph/0507711)

Balogh M. L., Christlein D., Zabludoff A. I., Zaritsky D., 2001, ApJ, 557, 117

Bell E. F., McIntosh D. H., Katz N., Weinberg M. D., 2003a, ApJL, 585, L117

Bell E. F., McIntosh D. H., Katz N., Weinberg M. D., 2003b, ApJS, 149, 289

Bell E. F., Naab T., McIntosh D. H., et al. 2005, ApJ accepted, (astro-ph/0506425)

Blanton M. R., Hogg D. W., Bahcall N. A., Baldry I. K., Brinkmann J., et al. 2003, ApJ, 594, 186

Blanton M. R., Lin H., Lupton R. H., Maley F. M., Young N., Zehavi I., Loveday J., 2003, AJ, 125, 2276

Cole S., Norberg P., Baugh C. M., Frenk C. S., Bland-Hawthorn J., et al. 2001, MNRAS, 326, 255

Colless M., Dalton G., Maddox S., Sutherland W., Norberg P., Cole S., Bland-Hawthorn J., et al. 2001, MNRAS, 328, 1039

Fioc M., Rocca-Volmerange B., 1997, A&A, 326, 950

Frith W. J., Shanks T., Outram P. J., 2005, MNRAS, 361, 701

Fukugita M., Shimasaku K., Ichikawa T., 1995, PASP, 107, 945

Graham A. W., Driver S. P., Petrosian V., Conselice C. J., Bershady M. A., Crawford S. M., Goto T., 2005, AJ, 130, 1535

Hogg D. W., Blanton M. R., Brinchmann J., Eisenstein D. J., Schlegel D. J., Gunn J. E., McKay T. A., Rix H.-W., Bahcall N. A., Brinkmann J., Meiksin A., 2004, ApJL, 601, L29

Jansen R. A., Franx M., Fabricant D., Caldwell N., 2000, ApJS, 126, 271

Jarrett T.-H., Chester T., Cutri R., Schneider S., Rosenberg J., Huchra J. P., Mader J., 2000, AJ, 120, 298

Jarrett T. H., Chester T., Cutri R., Schneider S., Skrutskie M., Huchra J. P., 2000, AJ, 119, 2498

Jarrett T. H., Chester T., Cutri R., Schneider S. E., Huchra J. P., 2003, AJ, 125, 525

Karachentsev I. D., Kutkin A. M., 2005, Astronomy Letters, 31, 299

Kauffmann G., Heckman T. M., White S. D. M., Charlot S., et al. 2003, MNRAS, 341, 33

Kochanek C. S., Pahre M. A., Falco E. E., Huchra J. P., Mader J., Jarrett T. H., Chester T., Cutri R., Schneider S. E., 2001, ApJ, 560, 566

Kochanek C. S., White M., Huchra J., Macri L., Jarrett T. H., Schneider S. E., Mader J., 2003, ApJ, 585, 161

Kron R. G., 1980, ApJS, 43, 305

Maller A. H., McIntosh D. H., Katz N., Weinberg M. D., 2003, ApJL, 598, L1

Maller A. H., McIntosh D. H., Katz N., Weinberg M. D., 2005,

ApJ, 619, 147
Nikolaev S., Weinberg M. D., Skrutskie M. F., Cutri R. M., Wheelock S. L., Gizis J. E., Howard E. M., 2000, AJ, 120, 3340
Pier J. R., Munn J. A., Hindsley R. B., Hennessy G. S., Kent S. M., Lupton R. H., Ivezić Ž., 2003, AJ, 125, 1559
Salzer J. J., Lee J. C., Melbourne J., Hinz J. L., Alonso-Herrero A., Jangren A., 2005, ApJ, 624, 661
Schlegel D. J., Finkbeiner D. P., Davis M., 1998, ApJ, 500, 525
Shectman S. A., Landy S. D., Oemler A., Tucker D. L., Lin H., Kirshner R. P., Schechter P. L., 1996, ApJ, 470, 172
Shimasaku K., Fukugita M., Doi M., Hamabe M., Ichikawa T., Okamura S., Sekiguchi M., Yasuda N., Brinkmann J., Csabai I., Ichikawa S., Ivezić Z., Kunszt P. Z., Schneider D. P., Szokoly G. P., Watanabe M., York D. G., 2001, AJ, 122, 1238
Sivakoff G. R., Saslaw W. C., 2005, ApJ, 626, 795
Skrutskie M. F., Schneider S. E., Stiening R., Strom S. E., Weinberg M. D., Beichman C., Chester T., Cutri R., Lonsdale C., Elias J., Elston R., Capps R., Carpenter J., Huchra J., Liebert J., Monet D., Price S., Seitzer P., 1997, in ASSL Vol. 210: The Impact of Large Scale Near-IR Sky Surveys The Two Micron All Sky Survey (2MASS): Overview and Status.. pp 25–+
Stoughton C., Lupton R. H., Bernardi M., Blanton M. R., Burles S., Castander F. J., Connolly A. J., Eisenstein D. J., Frieman J. A., Hennessy G. S., 2002, AJ, 123, 485
Strateva I., Ivezić Ž., Knapp G. R., Narayanan V. K., Strauss M. A., et al. 2001, AJ, 122, 1861
Strauss M. A., Weinberg D. H., Lupton R. H., Narayanan V. K., et al. 2002, AJ, 124, 1810
van Dokkum P. G., Franx M., Fabricant D., Kelson D. D., Illingworth G. D., 1999, ApJL, 520, L95
York D. G., Adelman J., Anderson J. E., Anderson S. F., Annis J., Bahcall N. A., Bakken J. A., Barkhouser R., Bastian S., Berman E., et al. 2000, AJ, 120, 1579

APPENDIX A: DEFINING OPTIMUM CRITERIA FOR MATCHING SDSS MAIN GALAXIES WITH 2MASS XSC COUNTERPARTS

For every MGS photometric source from DR2 we first find the nearest XSC source within a $60''$ radius. This allows us to characterise the criteria that we will use to construct the final XSC-MGS matched catalog of galaxies. Obviously, at larger angular separation $\theta_{\rm sep}$ between DR2 and XSC source centres there is an increased chance of multiple and random matches. The degree of this contamination in XSC-MGS cross correlation depends on magnitude and $\theta_{\rm sep}$. Since all galaxies follow a magnitude-size relation, such that brighter galaxies are larger on average, there is greater chance for a larger angular separation between the centres of DR2 and XSC cross-correlated sources.

We consider a multiple cross correlation to be two (or more) DR2 sources with the same XSC match. In the left panel of Figure A1, we plot the fraction of multiple sources per $\theta_{\rm sep}$ bin for different r-band magnitude limits. The multiple fraction increases more rapidly and at smaller angular separation for fainter magnitude cuts as a result of the increasing DR2 number counts. This behaviour continues until the final cut of $r > 17$ mag, at which point the XSC sources become so incomplete that the chance of even a random match at larger $\theta_{\rm sep}$ diminishes, making the observed multiple fraction flatten. Moreover, we illustrate the estimated fraction of random chance cross correlations per separation bin. The number of random sources $N_{\rm rand}$ is given by the probability of finding a XSC source in a given search area ($\pi\theta^2_{\rm sep}$) multiplied by the number of DR2 sources within that area. The probability of finding a random 2MASS XSC source in one square arcsecond is $3.58e-6$, given by 956,221 total sources over one half of the sky ($|b| \geq 30^\circ$). For example, there are 60,601 SDSS $16 < r \leq 17$ ($\mu_{50,r} \leq 23$) sources with $\theta_{\rm sep} \leq 3\farcs0$ resulting in 6 random matches, while there are only an additional 116 SDSS matches if we increase to $\theta_{\rm sep} \leq 4\farcs0$ and an additional 5 random matches or 4% random fraction for this bin. Similarly, there is roughly 2% random chance in the same interval for SDSS $14 < r \leq 15$ sources. We find that the random fraction contamination slowly diminishes at brighter magnitudes as a result of the lowering DR2 number counts.

In addition, we examine the distribution of nearest angular separation matches in the right panel of Figure A1. Here we plot the fraction of sources per $0\farcs25$ separation bin relative to the total number of sources with $\theta_{\rm sep} \leq 5\farcs0$ for different r-band magnitude intervals. All but the two brightest ($r < 13$ mag) intervals have identical angular separation distributions that peak around $\theta_{\rm sep} = 0\farcs5$, then fall quickly to < 1 percent at $\leq 1\farcs25$, and finally slowly drop to zero around $2\farcs0$. We see that a non-negligible fraction of the $r < 13$ mag sources have separations $> 1\farcs25$.

By combining the information in both panels of Figure A1 we can define an upper limit on the maximum angular separation per r-band magnitude interval that maximises the number of useful XSC-MGS cross-correlated sources and maximises contamination from multiple and random matches. For example, the left panel shows that multiple and random fractions for $r \leq 17$ and $r \leq 16$ are $< 1\%$ for $\theta_{\rm sep}$ of $1\farcs5$ and $2\farcs0$, respectively. For brighter magnitudes we see that larger separations are allowed before the contamination from multiple sources exceeds 1 percent. In columns 1–3 of Table A1, we tabulate the optimised angular separation cut per r-band magnitude interval, and the total number $N_{\rm cut}$ of matched sources therein. For the two bins brighter than $r = 13$ mag, we determine the best $\theta_{\rm sep}$ criteria by visual inspection of all matches within $60''$ radius.

In Table A1, we include the total counts from matching within other $\theta_{\rm sep}$ cuts ($5\farcs0$, $2\farcs0$, and $1\farcs25$), and an estimate of the number of multiple matches for several separations ($2\farcs0$, $3\farcs0$, and $5\farcs0$). For the magnitude bins brighter than $r = 15$, we visually confirm the optimally-matched sources with $\theta_{\rm sep} > 1\farcs25$. Recall that nearly all matches have separations less than $1\farcs25$ (Fig. A1, right panel). The number of sources between $1\farcs25$ and our optimised cut is given in column 10 of Table A1, and is the difference between columns 3 and 6. For $r \leq 15$ mag, this number is $> 1\%$ of $N_{\rm cut}$, and thus, warrants visual inspection.

In summary, we define a sliding angular separation cut that depends on raw r-band magnitude to achieve the most thorough catalog of XSC-MGS cross-correlated sources with negligible contamination from multiple and random matches. These criterion account for the extended nature of galaxies in the XSC. For matching SDSS main galaxies with 2MASS point sources, we search the PSC only for MGS sources not found in the XSC using a simple nearest match within a $2''$ radius (see §2.4).

This paper has been typeset from a TEX/ LATEX file prepared by the author.

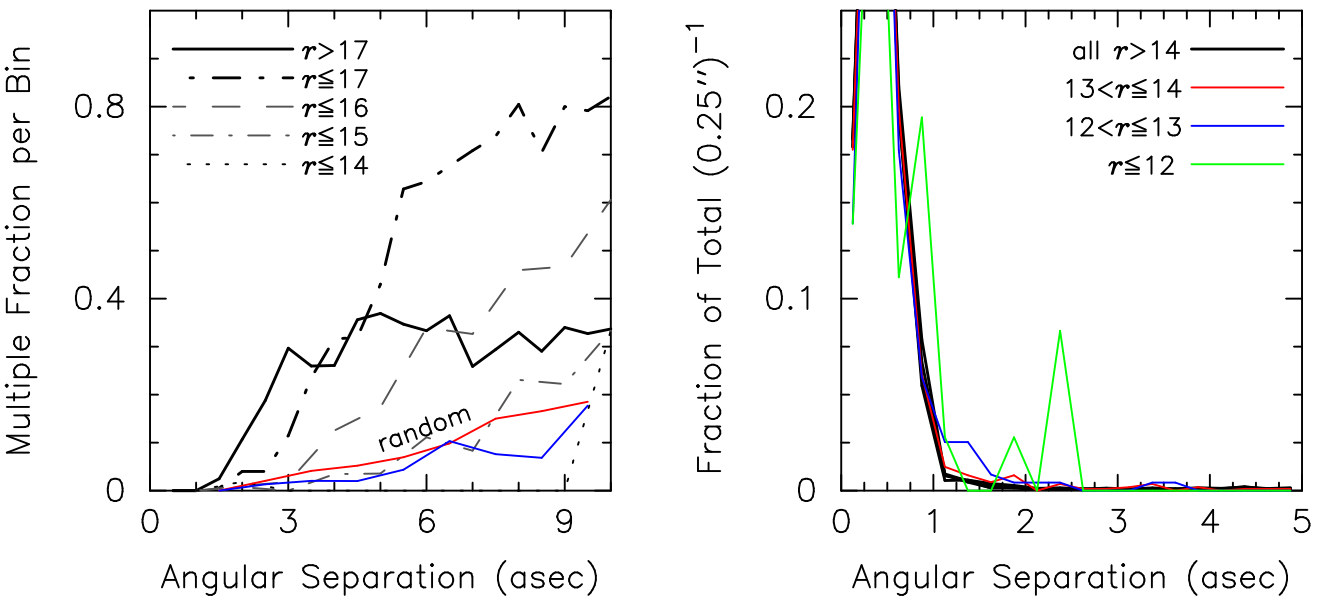

Figure A1. Multiple 2MASS XSC sources matched to individual SDSS MGS sources. Left: Fraction of multiple sources per angular separation bin for different r-band magnitude cuts (not extinction corrected). The $\theta_{\rm sep}$ bin size is $1\farcs0$ for $r \leq 16$ mag (bold lines) and $0\farcs5$ for $r > 16$ mag (thin lines). All sources have $\mu_{50,r} \leq 23$. In red ($16 < r \leq 17$) and blue ($14 < r \leq 15$), we estimate the number of random matches for the two r mag intervals. Right: For each r-band magnitude bin, we calculate the fraction of matched sources per $0\farcs25$ interval relative to the total number of cross-correlated sources within a $5''$ radius.

Table A1. XSC-MGS cross correlation.

mag bin	$\theta_{\rm sep}$ cut	$N_{\rm cut}$	N ($\leq 5\farcs0$)	N ($\leq 2\farcs0$)	N ($\leq 1\farcs25$)	$N_{\rm mult}$ ($\leq 2\farcs0$)	$N_{\rm mult}$ ($\leq 3\farcs0$)	$N_{\rm mult}$ ($\leq 5\farcs0$)	N ($1\farcs25$, cut)
(1)	(2)	(3)	(4)	(5)	(6)	(7)	(8)	(9)	(10)
$r \leq 12$	$30''$	40	36	33	32	0	0	0	8
$12 < r \leq 13$	$10''$	242	237	233	224	0	0	0	18
$13 < r \leq 14$	$4''$	1124	1127	1110	1087	1	1	1	37
$14 < r \leq 15$	$3''$	4853	4897	4832	4774	0	0	1	79
$15 < r \leq 16$	$2''$	19149	19335	19149	18959	4	6	12	190
$16 < r \leq 17$	$1\farcs5$	60267	60836	60432	59965	6	19	86	302
$r > 17$	$1\farcs25$	56106	57373	56548	56106	39	95	283	0

For the optimised XSC-MGS cross correlation per raw Petrosian r-magnitude intervals (1), we give the angular separation $\theta_{\rm sep}$ criteria between MGS and XSC source centres (2), and the resulting number of matched sources (3). The total number of matched sources using this set of criteria is 141,781 (sum of column 3). We provide total (4–6) and multiple (7–9) source counts for additional $\theta_{\rm sep}$ cuts. We visually inspect all optimally-matched sources (10) with $r \leq 15$ mag and $\theta_{\rm sep} > 1\farcs25$.